Title
Balancing Positive and Negative Selection: In Vivo Evolution of Candida lusitaniae MRR1

Journal
mBio, 12(2)

ISSN
2161-2129

Authors
Demers, Elora G
Stajich, Jason E
Ashare, Alix
et al.

Publication Date
2021-04-27

DOI
10.1128/mbio.03328-20

Peer reviewed

AMERICAN SOCIETY FOR MICROBIOLOGY | mBio®

RESEARCH ARTICLE

Balancing Positive and Negative Selection: *In Vivo* Evolution of *Candida lusitaniae MRR1*

Elora G. Demers,[a] Jason E. Stajich,[b] Alix Ashare,[c] Patricia Occhipinti,[a] Deborah A. Hogan[a]

[a]Department of Microbiology and Immunology, Geisel School of Medicine at Dartmouth, Hanover, New Hampshire, USA
[b]Department of Microbiology & Plant Pathology and Institute for Integrative Genome Biology, University of California—Riverside, Riverside, California, USA
[c]Dartmouth-Hitchcock Medical Center, Section of Pulmonary and Critical Care Medicine, Lebanon, New Hampshire, USA

ABSTRACT The evolution of pathogens in response to selective pressures present during chronic infections can influence their persistence and virulence and the outcomes of antimicrobial therapy. Because subpopulations within an infection can be spatially separated and the host environment can fluctuate, an appreciation of the pathways under selection may be most easily revealed through the analysis of numerous isolates from single infections. Here, we continued our analysis of a set of clonally derived *Clavispora* (*Candida*) *lusitaniae* isolates from a single chronic lung infection with a striking enrichment in the number of alleles of *MRR1*. Genetic and genomic analyses found evidence for repeated acquisition of gain-of-function mutations that conferred constitutive Mrr1 activity. In the same population, there were multiple alleles with both gain-of-function mutations and secondary suppressor mutations that either attenuated or abolished the constitutive activity, suggesting the presence of counteracting selective pressures. Our studies demonstrated trade-offs between high Mrr1 activity, which confers resistance to the antifungal fluconazole, host factors, and bacterial products through its regulation of *MDR1*, and resistance to hydrogen peroxide, a reactive oxygen species produced in the neutrophilic environment associated with this infection. This inverse correlation between high Mrr1 activity and hydrogen peroxide resistance was observed in multiple *Candida* species and in serially collected populations from this individual over 3 years. These data lead us to propose that dynamic or variable selective pressures can be reflected in population genomics and that these dynamics can complicate the drug resistance profile of the population.

IMPORTANCE Understanding microbial evolution within patients is critical for managing chronic infections and understanding host-pathogen interactions. Here, our analysis of multiple *MRR1* alleles in isolates from a single *Clavispora* (*Candida*) *lusitaniae* infection revealed the selection for both high and low Mrr1 activity. Our studies reveal trade-offs between high Mrr1 activity, which confers resistance to the commonly used antifungal fluconazole, host antimicrobial peptides, and bacterial products, and resistance to hydrogen peroxide. This work suggests that spatial or temporal differences within chronic infections can support a large amount of dynamic and parallel evolution and that Mrr1 activity is under both positive and negative selective pressure to balance different traits that are important for microbial survival.

KEYWORDS *Candida lusitaniae*, Mrr1, evolution, drug resistance, fluconazole, yeast, hydrogen peroxide, chronic infection, cystic fibrosis, *Candida albicans*, *Candida auris*

Understanding the positive and negative selective pressures that shape drug resistance profiles in microbial populations is critical for combating the development of antimicrobial resistance, an ever-increasing problem in clinical settings. Increased drug resistance in bacteria and fungi has been associated with clinically and agriculturally

Citation Demers EG, Stajich JE, Ashare A, Occhipinti P, Hogan DA. 2021. Balancing positive and negative selection: *in vivo* evolution of *Candida lusitaniae MRR1*. mBio 12: e03328-20. https://doi.org/10.1128/mBio.03328-20.

Editor James W. Kronstad, University of British Columbia

Address correspondence to Deborah A. Hogan, deborah.a.hogan@dartmouth.edu.

Received 25 November 2020
Accepted 4 February 2021
Published 30 March 2021

used antimicrobial agents (reviewed in references 1–3); however, drug resistance elements may also be selected for based on their ability to protect against factors produced by other microbes or plant, animal, and insect hosts (4, 5). Based on the analysis of bacterial isolates, such as *Burkholderia dolosa* or *Pseudomonas aeruginosa*, from single patients and across cohorts of patients, it is clear that *in vivo* factors can lead to the repeated selection for subpopulations with the same genes or pathways mutated (6–8). Similar studies have further shown that individual pathways can be upregulated and then downregulated in the same phylogenetic lineages. For example, suppressor mutations within *P. aeruginosa algU* frequently arise in strains already harboring mutations in the gene encoding the AlgU repressor MucA, which causes high AlgU signaling (9). Less is known about the negative selective pressures acting against sustained microbial resistance.

In the study by Demers et al. (10), we described a set of 20 recently diverged *Clavispora* (*Candida*) *lusitaniae* isolates obtained from the lung infection of a single individual with cystic fibrosis (CF). *C. lusitaniae* is among the emerging non-*albicans Candida* spp. that cause life-threatening disseminated infections in immunocompromised (11–13) and immunocompetent (14, 15) individuals. *C. lusitaniae* is notorious for its rapid development of resistance to antifungal drugs, including amphotericin B, azoles, and echinocandins (13, 16–19), which is interesting in light of its close phylogenetic relationship to *Candida auris* (20), a species in which multidrug-resistant isolates have caused hospital-associated outbreaks (21, 22). Our previous analyses of heterogeneity in fluconazole (FLZ) resistance among these isolates identified numerous distinct alleles of *MRR1* (*CLUG_00542*) (10). Multiple alleles encoded gain-of-function (GOF) mutations causing constitutive Mrr1 activity, which, as in other *Candida* species, increased expression of *MDR1* and Mdr1-dependent multidrug efflux pump activity (10, 23–30). At the time that these isolates were recovered, the patient had no history of antifungal treatment, suggesting that selection for constitutively active Mrr1 variants may have been driven by the need for resistance to other host- or microbe-produced compounds. Within this study, however, we found multiple lineages with recently evolved *MRR1* alleles that rendered cells more sensitive to FLZ than even *mrr1*Δ strains. Here, we address the perplexing question of why this population had recently diverged *MRR1* alleles that encoded both high and low Mrr1 activity. To do so, we expressed both native and synthesized *MRR1* alleles that represent intermediates during *MRR1* evolution in a common genetic background and tested the effects of these alleles on growth under *in vivo* relevant conditions. We concluded that multiple *C. lusitaniae MRR1* alleles conferring low Mrr1 activity resulted from an initial mutation that caused constitutive Mrr1 activity followed by a second mutation that either suppressed constitutive activation or inactivated the protein. Constitutive Mrr1 activity caused increased sensitivity to a variety of biologically relevant compounds, including hydrogen peroxide (H_2O_2), and suppression of constitutive Mrr1 activity rescued growth under some of these conditions. Monitoring populations from this subject's respiratory samples over time supports the model that there were opposing selective pressures *in vivo* that selected for and against constitutive Mrr1 activity, as reflected by the trade-off between FLZ and H_2O_2 resistance. These data provide insight into the persistence of a heterogeneous fungal population and underscores the complexity and parallelism of evolution that is possible in the human lung during a chronic infection.

RESULTS

Naturally evolved *C. lusitaniae MRR1* alleles confer altered Mrr1 activity and FLZ resistance. Each of the 20 closely related *C. lusitaniae* isolates from a single individual contained at least one nonsynonymous single nucleotide polymorphism (SNP) or single nucleotide insertion or deletion (indel) in *MRR1* relative to the deduced *MRR1* sequence of their most recent common ancestor (*MRR1*^{ancestral}), the sequence that resulted upon removing any of the SNPs that varied across the population (Fig. 1A) (10). While we did not identify any isolates with the *MRR1*^{ancestral} sequence in samples from this subject, we did find an isolate from another patient (B_L06) that contained

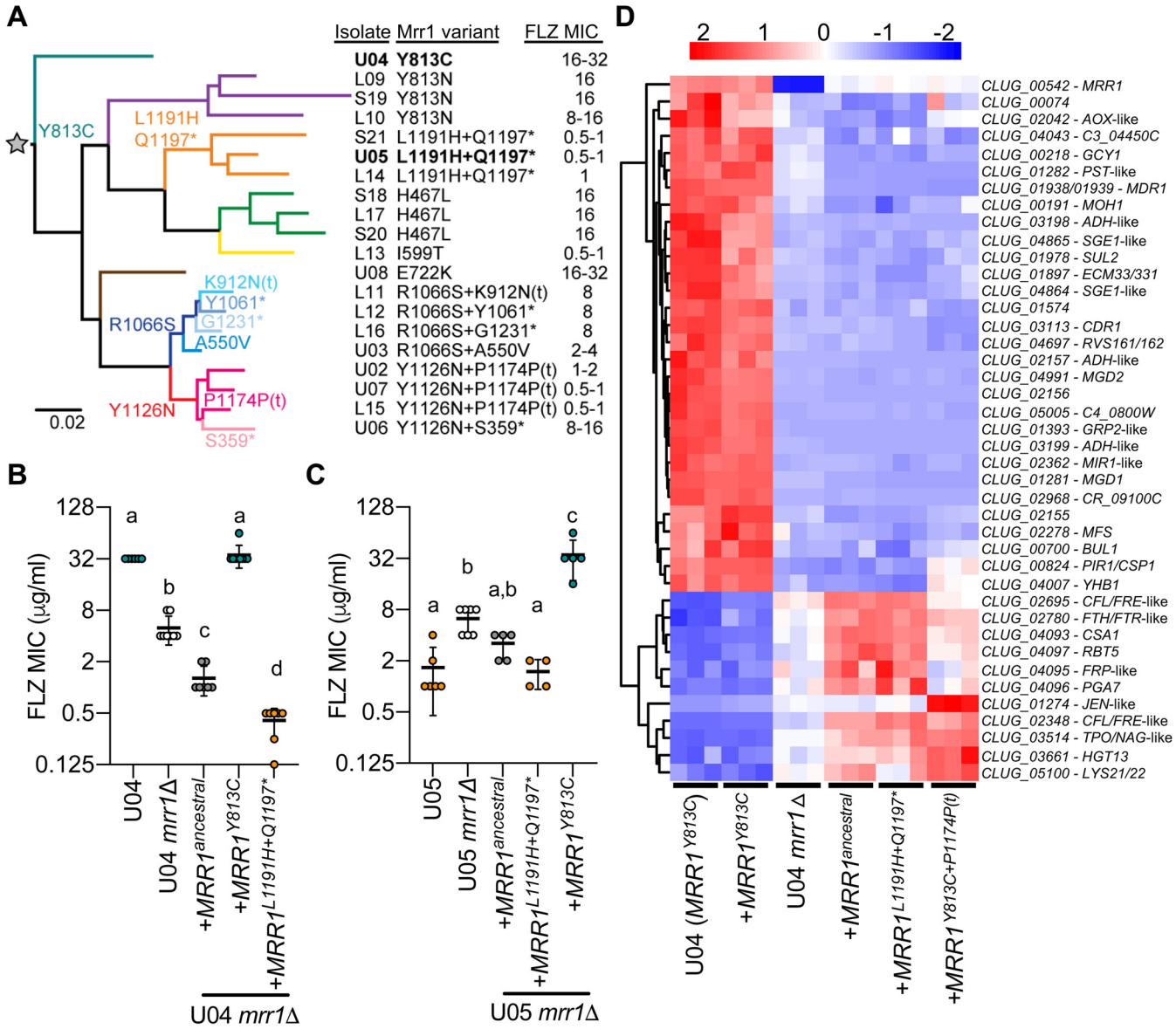

FIG 1 Constitutively active and low-activity Mrr1 variants naturally evolved in a single *C. lusitaniae* population. (A) Maximum likelihood-based phylogeny constructed from SNPs identified in the whole-genome sequences of 20 *C. lusitaniae* isolates; modified from Demers et al. (10). Select branchpoints are marked with the Mrr1 variants (text colored to match branches) present in subsequent isolates. Mrr1 variants are identified by amino acid changes that resulted from SNPs or indels; * indicates a stop codon. The one-nucleotide indel in codons P1174 (insertion) and K912 (deletion) cause frameshift mutations that resulted in early termination, denoted with "(t)," at N1176 and L927, respectively. Gray star at the root of the tree denotes the "ancestral" *MRR1* sequence, which lacks any of the mutations listed. U04 and U05, which are used in panels B and C, are highlighted. FLZ MICs (μg/ml) as determined in reference 10 are listed. (B) FLZ MICs for unaltered, *mrr1*Δ and *MRR1* complemented strains in the FLZ-resistant U04 (native allele $MRR1^{Y813C}$) strain background. (C) Same as in panel B, but in the FLZ-sensitive U05 strain background (native allele $MRR1^{L1191H+Q1197*}$). Strains containing the same *MRR1* allele in panels B and C are represented by circles of the same color. Data shown represent at least four independent assays on different days. Each sample was statistically compared to every other sample; the same lowercase letters indicate samples that are not significantly different, and different lowercase letters indicate significant differences ($P < 0.0001$ [B] or $P < 0.001$ [C]) as determined by one-way ANOVA with Tukey's multiple-comparison test of $\log_2$-transformed values. (D) Differentially expressed genes between strains harboring the constitutively active Mrr1-Y813C variant (U04 and U04 *mrr1*Δ+$MRR1^{Y813C}$) and those lacking *MRR1* (U04 *mrr1*Δ) or harboring low-activity variants (U04 *mrr1*Δ+$MRR1^{ancestral}$ and U04 *mrr1*Δ+$MRR1^{L1191H+Q1197*}$) when grown in liquid YPD medium; statistical cutoffs used were FDR of <0.05 and fold change of ≥2 (see Table S1 in the supplemental material). Normalized counts per million (CPM) from RNA-Seq are scaled by row (gene) with hierarchical clustering by Euclidean distance. Complemented strains are denoted by their respective *MRR1* allele. Predicted *C. albicans* homologs are listed next to *C. lusitaniae* gene names (Table S1).

the same sequence as the "$MRR1^{ancestral}$" allele. To determine the impact of specific mutations in *MRR1* on Mrr1 activity, we expressed different *MRR1* alleles in a common genetic background in which the native *MRR1* had been deleted (U04 *mrr1*Δ). Deletion of *MRR1* in the FLZ-resistant strain U04 reduced the FLZ MIC from 32 μg/ml to 4 μg/ml (10), and the decrease in MIC was complemented by restoring the native $MRR1^{Y813C}$

allele (Fig. 1B). We previously published that FLZ resistance in isolates from Fig. 1A correlated with expression of *MDR1* (10), also known as *MFS7* (19), and here show that deletion of *MDR1* similarly reduced the FLZ MIC of unaltered U04 and U04 *mrr1*Δ +*MRR1*^{Y813C} (8- to 16-fold) (see Fig. S1A in the supplemental material). Complementation of U04 *mrr1*Δ with the *MRR1*^{ancestral} allele resulted in a FLZ MIC of 1 μg/ml, 4-fold lower than the FLZ MIC of U04 *mrr1*Δ, suggesting that Mrr1^{ancestral} had a function that reduced the FLZ MIC (Fig. 1B). Expression of an *MRR1* allele from a closely related FLZ-sensitive isolate (*MRR1*$^{L1191H+Q1197*}$) reduced the FLZ MIC to 0.5 μg/ml (Fig. 1B). Similar relationships between the *MRR1* allele and FLZ MIC were observed when the *MRR1*^{ancestral}, *MRR1*^{Y813C}, and *MRR1*$^{L1191H+Q1197*}$ alleles were expressed in a *mrr1*Δ derivative of the FLZ-sensitive strain U05 (Fig. 1C); thus, further analyses were performed in the U04 background alone.

RNA-sequencing (RNA-seq) analysis validated the previously published result that *MDR1* expression paralleled FLZ MIC (Fig. 1D and Table S1) (10). Comparison of gene expression profiles for U04 (*MRR1*^{Y813C}), U04 *mrr1*Δ, and U04 *mrr1*Δ+*MRR1*^{Y813C} found that *mrr1*Δ was fully complemented upon return of *MRR1*^{Y813C} to the native locus (Fig. 1D and S2A) and confirmed that Mrr1 appears to both positively and negatively regulate a subset of genes (10, 29). Furthermore, a correlation analysis found that gene expression in U04 *mrr1*Δ+*MRR1*^{ancestral} and U04 *mrr1*Δ+*MRR1*$^{L1191H+Q1197*}$ was similar but distinct from that of the *mrr1*Δ strain (Fig. 1D and S2A). A linear model comparing these strains identified 41 genes with at least a 2-fold change in expression and corrected *P* value of $<$0.05. Comparison of nonisogenic *C. lusitaniae* strains similarly identified 22 of the genes in Table S1 as putatively Mrr1 regulated, including *MRR1* itself (10, 29). Eighteen genes were homologs or had similar predicted functions as genes previously published as regulated by *Candida albicans* Mrr1 (24), including *MDR1*, *FLU1*, and multiple putative methylglyoxal reductases encoded by *GRP2*-like genes, such as *MGD1* and *MGD2* (Fig. 1D and Table S1). Other genes within the Mrr1 regulon are discussed further below. These data indicate that the Mrr1-ancestral and Mrr1-L1191H+Q1197* variants had low basal activity, while Mrr1-Y813C was constitutively active.

The unexpected finding that FLZ MIC was higher upon deletion of *MRR1* than U04 expressing *MRR1*^{ancestral} or U05 was also observed in distantly related *C. lusitaniae* strains, ATCC 42720 and DH2383, with FLZ MICs of ~1 to 2 μg/ml (Fig. 1B and Fig. S1B). In both cases, deletion of *MRR1* led to a 2- to 4-fold increase in FLZ MIC (Fig. S1B). The elevated FLZ MIC in *mrr1*Δ strains was *MDR1* dependent, as the FLZ MIC was even lower in U04 *mrr1*Δ *mdr1*Δ than in U04 *mrr1*Δ (Fig. S1A). The increase was not due to introduction of the selectable marker *NAT1*, which encodes a nourseothricin acetyltransferase (31), as expression of *NAT1* from an intergenic site in the FLZ-sensitive U05 strain did not alter the FLZ MIC (Fig. S1C). These data led us to hypothesize that some Mrr1 variants (Mrr1-Y813C) caused constitutively high *MDR1* expression, while other Mrr1 variants (both Mrr1-ancestral and the recently diverged Mrr1-L1191H+Q1197*) repressed the expression of at least some Mrr1-controlled genes, such as *MDR1*. Indeed, the RNA-Seq analysis identified six genes, including *MDR1*, that while positively regulated when Mrr1 was constitutively active, were more highly expressed in U04 *mrr1*Δ than in those strains encoding low-activity Mrr1 variants (Fig. 1D and S2B). These data suggest that, for a small subset of Mrr1-regulated genes, including *MDR1*, low-activity Mrr1 variants may directly or indirectly inhibit expression. Cap1 (Clug_02670), another transcription factor known to regulate *MDR1* in *C. albicans* (32, 33), was not responsible for the increase in *MDR1* expression in the absence of *MRR1*, as deletion of *CAP1* from U05 *mrr1*Δ did not alter the FLZ MIC of this strain (4 to 8 μg/ml, $n = 3$).

Premature termination had varied effects on Mrr1 activity and inducibility in clinical isolates. Each of the 20 sequenced *C. lusitaniae* isolates contained *MRR1* alleles with either one or two nonsynonymous mutations relative to *MRR1*^{ancestral} (Fig. 1A), and we found that *C. lusitaniae* isolates with two mutations in *MRR1* had a significantly lower average FLZ MIC than isolates with a single *MRR1* mutation (Fig. 2A). Interestingly, six of

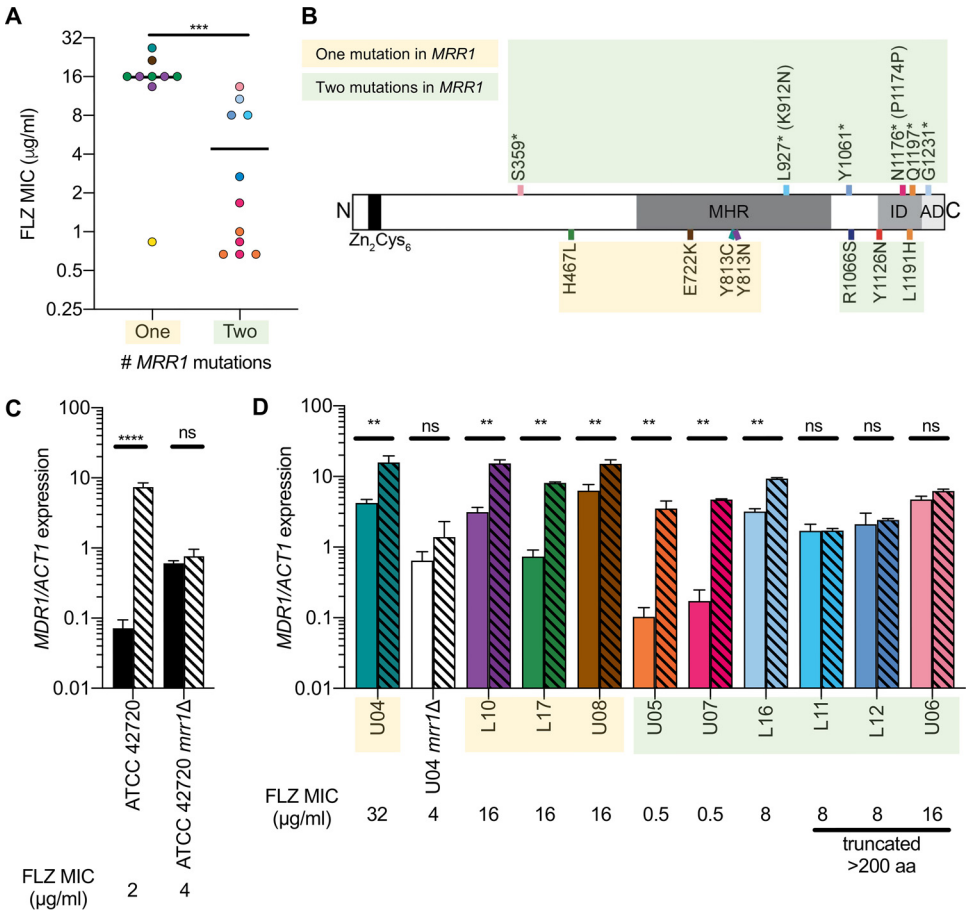

FIG 2 Premature stop codons in Mrr1 differentially impact *MDR1* induction by benomyl. (A) Mean FLZ MICs for each of the 20 clinical *C. lusitaniae* isolates in Fig. 1A separated by the number of nonsynonymous mutations within *MRR1* (as defined in reference 10); mean of each group is shown. Two-tailed unpaired *t* test of $\log_2$-transformed MIC values; ***, $P < 0.001$. (B) Schematic of *C. lusitaniae MRR1* annotated with putative regulatory domains determined by sequence analysis and homology to *C. albicans* (22) and locations of truncating (top) and putative activating (bottom) mutations. Putative domains include a DNA binding domain with a zinc cluster motif (Zn_2Cys_6; amino acids 33 to 61), a transcriptional regulatory middle homology region (MHR; amino acids ~607 to 1023), an inhibitory domain (ID; amino acids 1123 to 1217), and an activating domain (AD; amino acids 1218 to 1265). L927 and N1176 are the locations of stop codons caused by indels in codons K912 and P1174, respectively. (C and D) *MDR1* expression normalized to *ACT1* in the absence (solid bars) or presence (striped bars) of 50 μg/ml benomyl. Means ± standard deviations (SDs) of representative data in biological triplicates are shown; similar trends observed on at least three different days. Two-way ANOVA with Sidak's multiple-comparison test; **, $P < 0.01$; ****, $P < 0.0001$; ns, not significant. In panel D, strain names are highlighted corresponding to the number of mutations in *MRR1*, yellow for one and green for two, as in Fig. 2B. The colors of the circles (A), lines (B), and bars (D) correspond to *MRR1* alleles shown Fig. 1A.

the seven *MRR1* alleles in the "two-mutation" set had premature stop codons, resulting in the loss of 34 to 906 amino acids (Fig. 2B). There were two instances in which the same mutation was found in combination with different nonsense mutations (*) or single nucleotide indels that led to early termination (t): $MRR1^{\mathbf{Y1126N}+P1174P(t)}$ or $MRR1^{\mathbf{Y1126N}+S359\mathbf{*}}$ and $MRR1^{\mathbf{R1066S}+K912N(t)}$, $MRR1^{\mathbf{R1066S}+Y1061\mathbf{*}}$, or $MRR1^{\mathbf{R1066S}+G1231\mathbf{*}}$ (common mutations in bold) (Fig. 1A). This suggested a complex evolutionary history for these alleles.

To better understand the effects of mutations in *MRR1* on Mrr1 activity, we analyzed the effects of a chemical inducer of Mrr1 activity, benomyl (24, 34, 35), on *MDR1* expression. Benomyl strongly induced *MDR1* expression in an Mrr1-dependent manner in the FLZ-sensitive strain ATCC 42720 (Fig. 2C) and, to a lesser extent, in the FLZ-resistant strain U04, which had high basal *MDR1* expression (Fig. 2D). Quantitative reverse transcription-PCR (qRT-PCR) analysis of *MDR1* expression and induction by benomyl in

this collection of clinical isolates with different Mrr1 variants found that the two isolates with the lowest basal *MDR1* expression and lowest FLZ MIC (U05 and U07) had the greatest induction by benomyl (34- and 27-fold, respectively) (Fig. 2D), suggesting that despite the loss of 68 or 89 amino acids, respectively, they encoded functional but low-activity Mrr1 variants. Three isolates, L11, L12, and U06, had intermediate FLZ MICs and *MDR1* expression levels but did not show benomyl induction, similar to *mrr1*Δ strains (Fig. 2C and D). These strains all encoded Mrr1 variants lacking greater than 200 amino acids, suggesting that these mutations caused a loss of Mrr1 function. Isolate L16, which encoded two mutations in Mrr1 but only lacked 34 amino acids from the C terminus, phenocopied strains with a single mutation in *MRR1*, such as U04, L10, L17, and U08, suggesting either removal of a C-terminal regulatory region or that the mutation not causing premature termination increased Mrr1 activity (Fig. 2D).

Premature stop codons repeatedly arose in constitutively active Mrr1 variants and caused either a loss of constitutive Mrr1 activity or a complete loss of Mrr1 function. In light of the mixed effects that these two-mutation *MRR1* alleles had on Mrr1 activity, we sought to determine the individual effects of mutations within each allele with a focus on the two strains with the lowest basal *MDR1* expression and the strongest induction of *MDR1* in response to benomyl, $MRR1^{L1191H+Q1197*}$ (in U05) (Fig. 3A) and $MRR1^{Y1126N+P1174P(t)}$ (in U07) (Fig. 3B). We found that the $MRR1^{L1191H}$ mutation caused a 32-fold increase in FLZ MIC (Fig. 3C) and 22-fold increase in *MDR1* expression (Fig. 3D) compared to that for $MRR1^{ancestral}$, indicating that, like the Mrr1-Y813C variant, Mrr1-L1191H was constitutively active. In contrast, $MRR1^{Q1197*}$, which caused the loss of 68 amino acids from the C terminus of Mrr1, did not significantly alter the FLZ MIC compared to that for the $MRR1^{ancestral}$ allele, suggesting that it was neither a constitutively activating nor null mutation (Fig. 3C). The combination of mutations in $MRR1^{L1191H+Q1197*}$ resulted in a 128-fold decrease in FLZ MIC (Fig. 3C) and 38-fold decrease in *MDR1* expression (Fig. 3D) compared to that for a strain expressing $MRR1^{L1191H}$, phenotypes that mirrored the strain expressing $MRR1^{ancestral}$.

$MRR1^{Y1126N+P1174P(t)}$ (from U07) and $MRR1^{Y1126N+S359*}$ (from the closely related U06) (Fig. 1A), were similarly analyzed (Fig. 3B). Expression of $MRR1^{Y1126N}$ in U04 *mrr1*Δ caused high FLZ resistance (MIC of 32 to 64 μg/ml) (Fig. 3C) and *MDR1* expression (Fig. 3D), similar to that for strains with $MRR1^{Y813C}$ or $MRR1^{L1191H}$. Addition of the frameshift-inducing indel at P1174, which causes a premature stop codon at N1176 removing 89 amino acids, yielding $MRR1^{Y1126N+P1174P(t)}$, caused a 128-fold decrease in FLZ MIC and >100-fold decrease in *MDR1* expression relative to that for the strain expressing $MRR1^{Y1126N}$, again leading to a strain that phenocopied one expressing $MRR1^{ancestral}$ (Fig. 3C and D). The addition of the indel at P1174 to an allele with a different constitutively active variant, creating $MRR1^{Y813C+P1174P(t)}$, similarly caused 256- and >100-fold decreases in FLZ MIC and *MDR1* expression, respectively, relative to that for a strain expressing the $MRR1^{Y813C}$ allele (Fig. 3C and D). Further RNA-Seq analysis of U04 *mrr1*Δ+$MRR1^{Y813C+P1174P(t)}$ showed decreased expression of many genes positively regulated by Mrr1 (Fig. 1D). In contrast, addition of a SNP causing an early stop codon at S359 to the allele with the activating Y1126N mutation ($MRR1^{Y1126N+S359*}$) yielded a strain that phenocopied U04 *mrr1*Δ, indicating this variant, lacking 906 amino acids from the C terminus, was inactive (Fig. 3C and D). Together, these data show that the Y1126N mutation, which arose first, caused constitutive Mrr1 activity that was subsequently suppressed by premature stop codons that either restored low activity [P1174P(t)] or eliminated activity (S359*).

In addition to the differences in basal activity, the individual mutations alone and in combination affected chemical inducibility by benomyl. Levels of *MDR1* were strongly induced by benomyl in U04 *mrr1*Δ+$MRR1^{ancestral}$ (40-fold increase) but not in the U04 parental strain with high Mrr1 activity or its *mrr1*Δ derivative (Fig. 3D). The three constitutively active variants (Mrr1-Y813C, Mrr1-L1191H, and Mrr1-Y1126N) showed only a 2- to 3-fold increase in *MDR1* expression with benomyl (Fig. 3D), similar to what was observed for FLZ-resistant clinical isolates (Fig. 2D). Surprisingly, addition of mutations that caused premature stop codons within the last 100 amino acids of Mrr1 to the

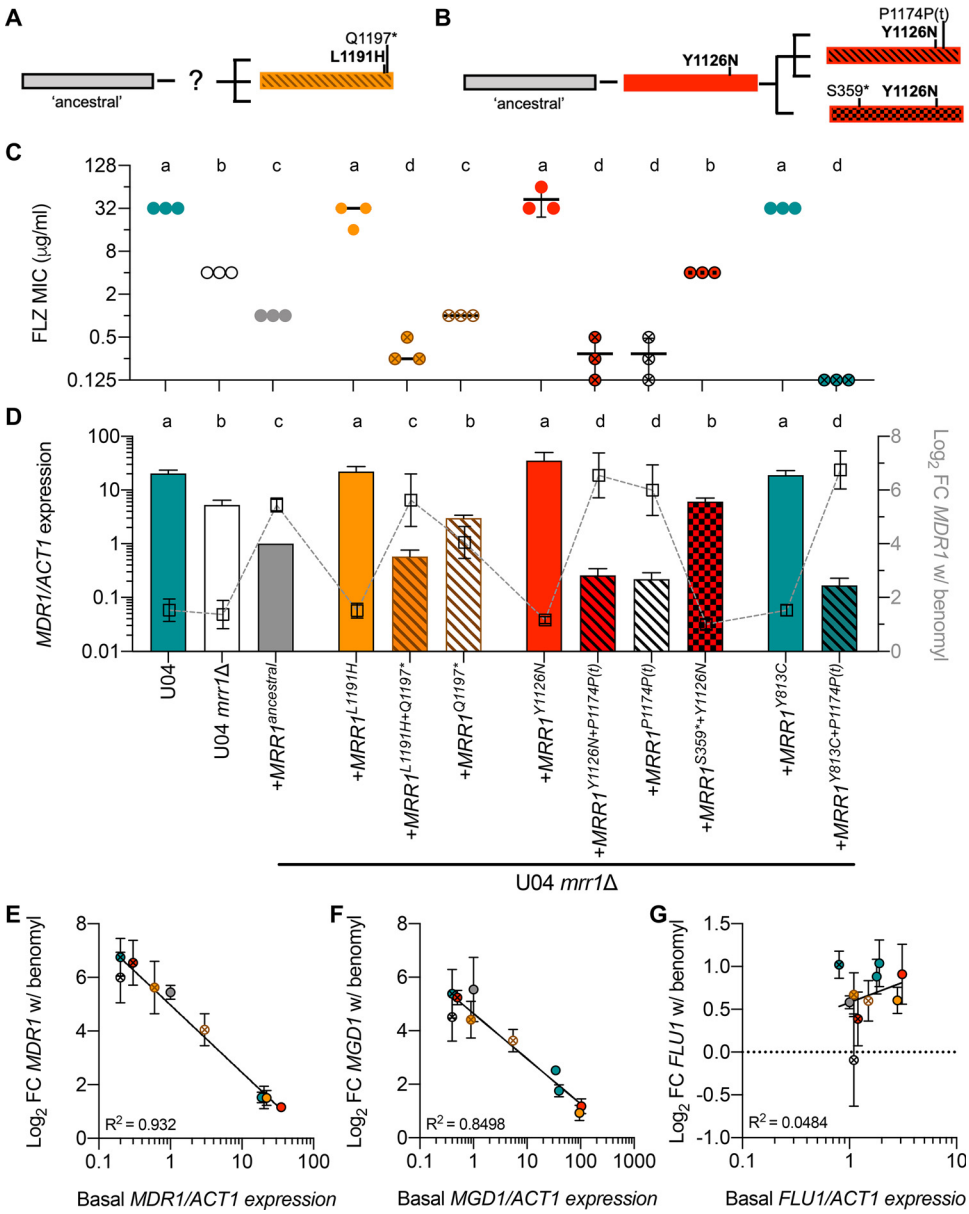

FIG 3 Premature stop codons repeatedly arose in constitutively active Mrr1 variants resulting in reduced Mrr1 activity but, in some cases, restored Mrr1 inducibility. Schematic of inferred evolution of *MRR1* alleles in the L1191H+Q1197* (A) and Y1126N (B) lineages. (C) FLZ MICs for U04, U04 *mrr1*Δ and *MRR1* complemented strains in the U04 *mrr1*Δ background. Means ± SDs from three independent assays on different days shown. Each sample was statistically compared to every other sample; the same lowercase letters indicate samples that are not significantly different, and different lowercase letters indicate significant differences ($P < 0.01$) as determined by one-way ANOVA with Tukey's multiple-comparison test of $\log_2$-transformed values. (D) *MDR1* expression normalized to *ACT1* from culture grown in YPD (bars, left *y* axis). Means ± SDs from three independent assays on different days; data from each day were normalized to the expression of U04 *mrr1*Δ+*MRR1*^{ancestral}. Each sample was statistically compared to every other sample; the same lowercase letters indicate samples that are not significantly different, and different lowercase letters indicate significant differences (b to d, $P < 0.05$; all other pairwise comparisons, $P < 0.01$) as determined by one-way ANOVA with Tukey's multiple-comparison testing of $\log_2$-transformed data. Overlaid with $\log_2$-transformed mean ± SD fold change (FC) in normalized *MDR1* expression following exposure to 50 μg/ml benomyl (squares, right *y* axis); full data presented with statistics in Fig. S3D. (C and D) FLZ MICs and *MDR1/ACT1* expression data are colored to match; the sample names are shown on the *x* axis of panel D. Comparison of mean basal *MDR1* (E), *MGD1* (F), or *FLU1* (G) expression from panel D and Fig. S3B or C, respectively, excluding strains lacking functional *MRR1*, and mean ± SD $\log_2$-transformed FC of the induction following benomyl exposure from Fig. S3D to F; circles colored to match those in panel C. Goodness of fit r^2 value for nonlinear regression shown.

constitutively active variants restored inducibility by benomyl (Fig. 3D). In fact, there was a significant inverse correlation between basal *MDR1* expression and fold induction by benomyl (Fig. 3E).

As in *C. albicans*, *C. lusitaniae* Mrr1 regulates the expression of the methylglyoxal reductase encoded by *MGD1* (*CLUG_01281* or *GRP2*) (10, 24, 29, 36, 37) and the multidrug efflux pump encoded by *FLU1* (*CLUG_05825*) (10, 29, 38, 39) (Table S1 and Fig. S3A). As with *MDR1*, expression of both *MGD1* and *FLU1* was significantly higher in strains encoding constitutively active variants than in a strain encoding the Mrr1 ancestral variant, and the absence of the C terminus in strains with activating mutations caused a significant decrease in basal expression (Fig. S3B and S3C). Benomyl induction of *MGD1*, like that of *MDR1* (Fig. S3D), was restored upon loss of the C terminus from constitutively active Mrr1 variants, further supporting the strong negative correlation between basal expression and benomyl inducibility (Fig. 2F and Fig. S3E). *FLU1* expression, however, was not induced by benomyl in any strain, suggesting that *FLU1* regulation by Mrr1 differs from *MGD1* and *MDR1* regulation (Fig. 2G and Fig. S3F). Furthermore, *MDR1* and *MGD1* were both derepressed in the absence of Mrr1 (Fig. 1D and Fig. S2B), while *FLU1* was not and was only weakly differentially expressed between strains with constitutive and low Mrr1 activity ($<$2-fold) (Fig. S3C). Together these data indicate the C terminus of Mrr1 is required for constitutive expression of multiple Mrr1-regulated genes but not for benomyl induction of the Mrr1-regulated genes tested (Fig. S3A). Combined with the Mrr1 activity across clinical isolates (Fig. 2D), these data indicate that in some strains with constitutively active Mrr1 variants, there was repeated selection for mutations to decrease Mrr1 activity, resulting in a mixed population containing constitutively active, prematurely terminated but inducible and loss-of-function (LOF) Mrr1 variants.

Constitutive Mrr1 activity negatively impacts H_2O_2 resistance. We next sought to understand why mutations that reduce Mrr1 activity might repeatedly arise in this chronic infection. Previous studies have shown that overexpression of drug efflux pumps in drug-resistant microbes can cause a fitness defect due to the energetic cost of constitutive pump production and activity in the absence of a selective substrate (40–42). Deletion of *MDR1* from U04 *mrr1*Δ+*MRR1*^{Y813C}, which constitutively expresses *MDR1*, however, did not alter the growth kinetics (Fig. 4A). In the absence of an obvious growth defect, we considered factors present in the CF lung, which has been characterized as a highly inflamed environment containing elevated levels of neutrophils, macrophages, and oxidative stress (reviewed in references 43 and 44). Although little is known about fungus-dominated chronic lung infections in CF, such as the infection from which these isolates were obtained, an analysis of cytokines within the bronchoalveolar lavage (BAL) fluid from the patient these isolates originated from showed proinflammatory cytokines (interleukin 8 [IL-8] and IL-1β) present were consistent with the neutrophilic environment seen in other patients with CF (Fig. 4B) (44).

In light of these findings, we investigated the effects of Mrr1 activity on reactive oxygen species (ROS) stress generated by H_2O_2, a stress strongly associated with high neutrophil counts. In a serial dilution assay, we found that isogenic strains harboring constitutively active Mrr1 variants, while resistant to FLZ and diamide (Fig. S4A), had increased sensitivity to 4 mM H_2O_2 compared to that of one harboring the Mrr1 ancestral variant (Fig. 4C). Diamide was used to illustrate relative Mrr1 activity instead of FLZ, because serial dilution assays on rich medium (yeast-peptone-glucose [YPD]) containing FLZ are not always representative of FLZ MIC, which are assessed in defined medium (Fig. S4B). Secondary mutations resulting in either a phenotype associated with low Mrr1 activity that is inducible or a complete loss of Mrr1 activity both restored H_2O_2 resistance to levels similar to that of strains harboring the Mrr1 ancestral variant (Fig. 4C; Fig. S4A). The effects of Mrr1 activity on H_2O_2 sensitivity were similar among isogenic strains in both the U04 and U05 backgrounds (Fig. 4C and Fig. S4B). Surprisingly, deletion of *MDR1* from strains harboring the constitutively active Mrr1-Y813C variant partially rescued growth (Fig. S4A); however, the absence of *MDR1* did

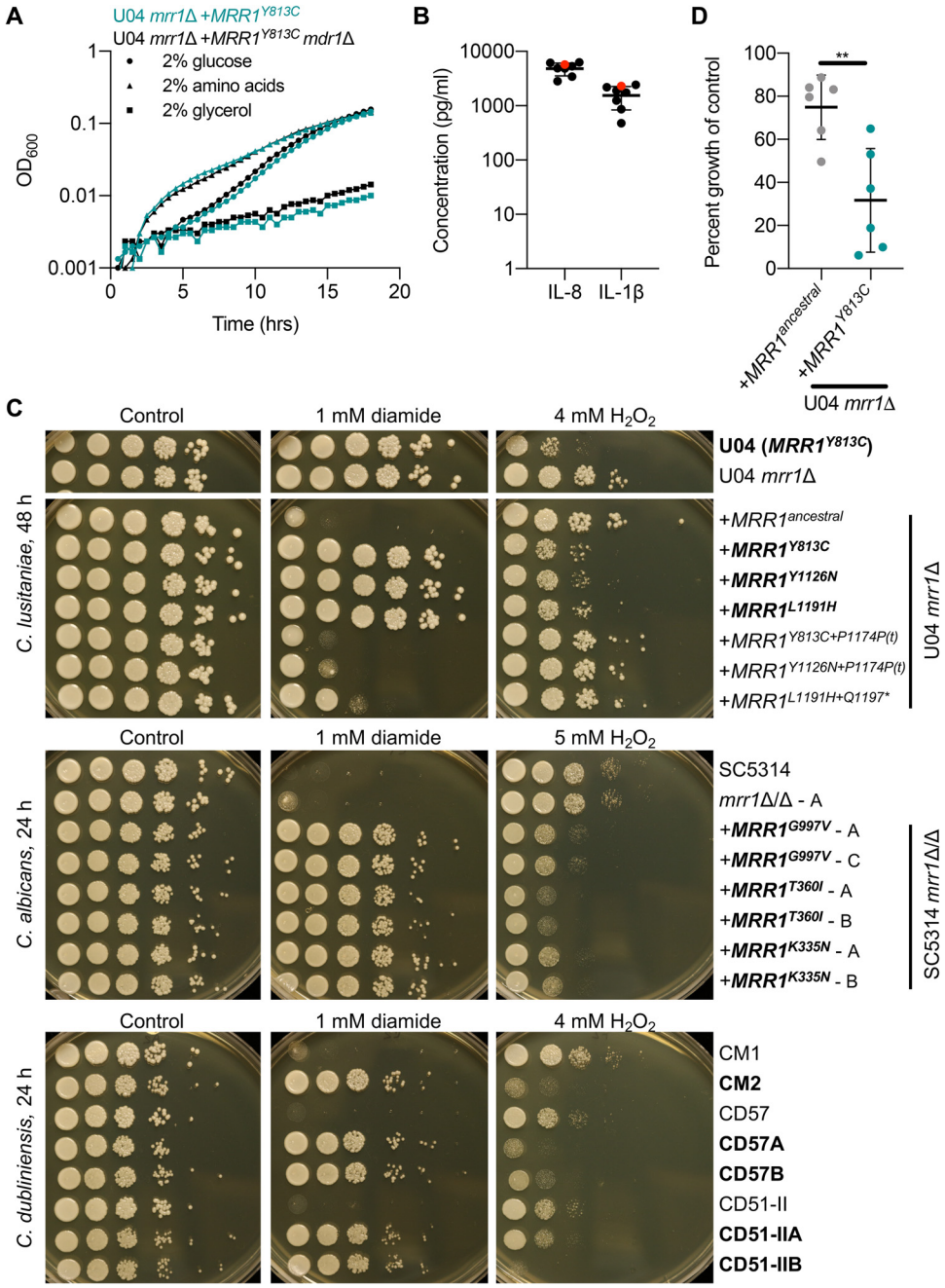

FIG 4 Constitutive Mrr1 activity decreases resistance to H_2O_2 in multiple *Candida* species. (A) Growth curve of U04 *mrr1*Δ+*MRR1*^{Y813C} (teal) and U04 *mrr1*Δ+*MRR1*^{Y813C} *mdr1*Δ (black) grown at 37°C in YNB medium supplemented with the indicated carbon source: glucose (circles), amino acids (triangles), or glycerol (squares). Means from representative data acquired in triplicates shown. (B) Quantification of cytokines IL-8 and IL-1β in BAL fluid from the CF patient with (red) or seven patients without (black) *C. lusitaniae* in their lungs. Two-way ANOVA with Sidak's multiple-comparison testing found no significant differences. (C) Serial dilution assays of *C. lusitaniae*, *C. albicans*, and *C. dubliniensis* strains on YPD or YPD supplemented with the indicated concentration of diamide or H_2O_2. Strain names in bold font were shown to contain GOF mutations in Mrr1 resulting in increased FLZ resistance (Fig. 3C and references 39, 45, and 46). Plates were imaged after 24 or 48 h of growth at 37°C, as indicated. (D) Percent growth in well-aerated 5 ml YPD plus 1 mM H_2O_2 was calculated relative to that of the vehicle only control after 22 to 24 h growth at 37°C. These data represent six independent assays performed on different days. Significance determined by paired *t* test; **, $P < 0.01$.

not completely explain the differences, as strains lacking *MRR1* had increased H_2O_2 resistance despite elevated *MDR1* expression (Fig. 4C). Additionally, the double mutant U04 *mrr1*Δ *mdr1*Δ did not have increased resistance to H_2O_2 compared to that of U04 *mrr1*Δ (Fig. S4A) suggesting this may be a complex response. A secondary assay quantifying growth after ~24 h in liquid cultures containing 1 mM H_2O_2, though variable day to day, confirmed there was a reproducible difference in growth between strains harboring the low-activity Mrr1 ancestral and constitutively active Mrr1-Y813C variants (Fig. 4D). To determine if this phenomenon was unique to *C. lusitaniae*, we examined a set of isogenic *C. albicans* isolates (39) and *in vivo*- or *in vitro*-evolved *Candida dubliniensis* isolates (25) expressing *MRR1* alleles containing GOF mutations. We found that for all *C. albicans* and *C. dubliniensis* strain sets tested, strains with high Mrr1 activity, which had increased FLZ (39, 45, 46) and diamide resistance, were more sensitive to H_2O_2 than strains with low Mrr1 activity or lacking *MRR1* (Fig. 4C). As in *C. lusitaniae*, deletion of *MDR1* restored growth on H_2O_2 in *C. albicans* (Fig. S4C). These data show that the Mrr1 activity-driven trade-off between FLZ and H_2O_2 resistance is conserved across multiple *Candida* species.

A screen of isogenic *C. lusitaniae* strains for growth in various concentrations of 48 chemical compounds resuspended from the Biolog Phenotype MicroArray microplates (Fig. S5) supported our findings that constitutive Mrr1 activity can increase sensitivity to oxidative stress. When comparing strains harboring either the low-activity Mrr1 ancestral variant or the constitutively active Mrr1-Y813C variant, with either *MDR1* intact or removed, we found there were minimal differences in growth in the medium used to resuspend the Biolog compounds (Fig. S5A), and many conditions caused less than a 25% difference in growth. Unsurprisingly, constitutive Mrr1 activity conferred Mdr1-dependent resistance to 12 compounds, including three triazoles (FLZ, propiconazole, and myclobutanil) (Fig. S5B and C). High Mrr1 activity also led to Mdr1-independent resistance to four additional compounds, including two additional azoles (3-amino-1,2,4-triazole and miconazole nitrate) (Fig. S5B and C). Eight compounds caused a largely Mdr1-independent decrease in growth in strains harboring the constitutively active Mrr1-Y813C variant: 6-azauracil, berberine, BAPTA, lithium chloride, aminacrine, sodium metasilicate, pentamidine isethionate, and potassium chromate (Fig. S5D). Though diverse, these compounds have been reported to have varied effects on microbial metabolism or respiration (47–53) and/or alter DNA/RNA integrity (54–59) directly or indirectly through oxidative damage. Interestingly, berberine and calcium inhibitors, such as BAPTA, have previously been shown to alter growth of antifungal-resistant *Candida* species (60–62). Strains lacking *MRR1* or harboring the low-activity Mrr1-L1191H+Q1197* variant were not as sensitive to some of these compounds, supporting our findings that secondary mutations causing a decrease or loss of Mrr1 activity can restore resistance in some oxidative stress environments (Fig. S5D).

To gain insight into the mechanisms that lead to differences in oxidative stress resistance between strains with different levels of Mrr1 activity, we compared the gene expression profiles after a 30-min exposure to 0.5 mM H_2O_2, a partially inhibitory concentration. H_2O_2 exposure had broad strain-independent effects on the transcriptome, altering expression of 786 genes (fold change [FC] $\geq$ 2, false-discovery rate [FDR] $<$ 0.05), including increased expression of *CLUG_04072*, a homolog of *C. albicans* catalase (*CAT1*), which was previously shown to be important for the resistance of *C. lusitaniae* to H_2O_2 (63) (see Fig. S6A and Table S2). While there were subtle differences in the H_2O_2 response between strains expressing the constitutively active Mrr1-Y813C variant compared to U04 *mrr1*Δ+*MRR1*^{ancestral}, there were no clear patterns that would explain the difference in H_2O_2 resistance (Fig. S6B). The majority of differences in gene expression were seen in the magnitude of induction of Mrr1-regulated genes by H_2O_2, a known inducer of Mrr1 in other species (24, 32) (Fig. S6B and C; Table S2). We analyzed the expression of homologs of oxidative stress response (OSR) genes previously characterized in *C. albicans* (*Ca*) and *Saccharomyces cerevisiae* (*Sc*) and found that there was not a significant Mrr1-dependent difference in basal or H_2O_2-induced expression of these genes (Fig. S6A). Genes

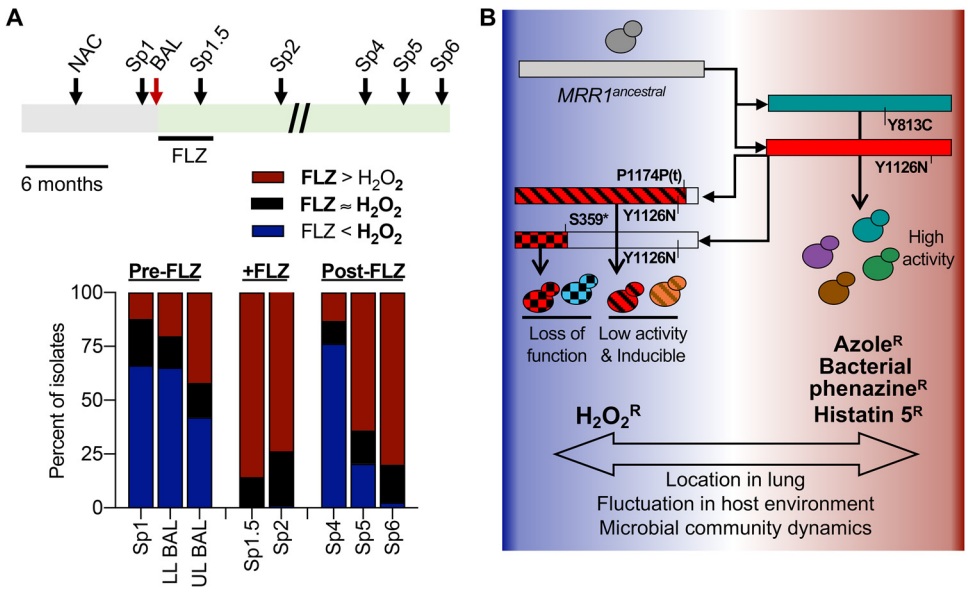

FIG 5 Trade-off between FLZ and H_2O_2 resistance persists in evolving *C. lusitaniae* populations during a chronic lung infection. (A) Schematic of sampling timeline (top) and histogram of the number of isolates that (i) were mostly uninhibited on FLZ, but were inhibited by H_2O_2 (red), (ii) were mostly uninhibited on H_2O_2 but were inhibited by FLZ (blue), or (iii) were uninhibited under both conditions (black). For the schematic, the gray bar represents the 6 to 10 months before the BAL during which this patient was identified as being colonized by non-*albicans Candida* (NAC) species. *C. lusitaniae* was determined to be the dominate microbe in the upper and lower lobe (UL and LL, respectively) BAL samples (red arrow), which marks the start of the green bar. Sp1 was obtained 1 month before the BAL and was retrospectively also found to contain abundant *C. lusitaniae*. Sp1.5, Sp2, Sp4, Sp5, and Sp6 were obtained 3, 9, 32, 35, and 38 months, respectively, after the BAL and all contained *C. lusitaniae*. A 4-month course of FLZ therapy was given after the BAL. Scale bar indicates 6 months. Multiple isolates were collected from each sample/timepoint (n = 38 to 80) and assayed for growth on YPD supplemented with 8 μg/ml FLZ or 4 mM H_2O_2. Growth was scored as completely inhibited, partially inhibited or uninhibited compared to that of a YPD-only control. (B) Model for the evolution of *C. lusitaniae MRR1* in this population. Whole-genome sequencing and mutation analyses suggest that following the initial infection with *C. lusitaniae* harboring the Mrr1-ancestral variant, a combination of exposure to different stimuli that changed overtime or by locations within the CF lung environment led to the selection for a heterogeneous population. Multiple constitutively active Mrr1 variants arose, and while some persisted over time, others were subsequently mutated again. The secondary mutations causing premature stop codons (represented by shortened bars) resulted in reversion to low Mrr1 activity that was inducible or complete loss of Mrr1 activity. The balance between selective pressures resulted in a heterogeneous population of isolates with varied resistance (^{R}) to biologically and clinically important compounds.

assessed included the OSR transcription factor encoded by *CaCAP1* or *ScYAP1*, superoxide dismutase (*SOD2*, *SOD4*, and *SOD6*), enzymes involved in the thioredoxin (*TSA1*, *TRX1*, and *TRR1*) and glutathione (*GPX* and *GSH1*) systems, catalases, and OSR genes involved in carbohydrate metabolism and the DNA-damage response (64, 65). Further analysis is required to better understand the link between constitutive Mrr1 activity and H_2O_2 sensitivity; however, these data highlight that the sensitivity is not due to failure to induce an oxidative stress response but is more likely a consequence of Mrr1-regulated genes, such as *MDR1*.

Phenotype dynamics in chronic infection populations over time. In light of the evidence for complex evolution of *MRR1* and the potentially advantageous phenotypes associated with both high and low Mrr1 activity, we sought to better understand the fraction of isolates with these Mrr1-associated traits over time. For this analysis we used arrayed *C. lusitaniae* populations isolated from one BAL procedure sample or from sputum collected from the same subject over 3 years, with the first time point approximately 6 months after the first clinical culture report of the high levels of "non-*albicans Candida*" as shown in Fig. 5A. When screening isolates for growth on FLZ (8 μg/ml) or H_2O_2 (4 mM), we found an inverse correlation between growth on FLZ and growth on H_2O_2 (Fig. 5A). It was uncommon for isolates to be uninhibited under both

conditions. Isolates from the early samples were predominately sensitive to FLZ (10) and resistant to H_2O_2. During and soon after the course of FLZ therapy (Sp1.5 and Sp2, respectively), however, there was an increase in isolates that were FLZ resistant and H_2O_2 sensitive (Fig. 5A). Subsequent samples from 2 years after the FLZ therapy was completed varied in the proportion of isolates that grew better on H_2O_2 and FLZ. Thus, over the course of 3 years, we repeatedly identified isolates that were either FLZ resistant and H_2O_2 sensitive, or vice versa, but not typically resistant to both, further supporting a trade-off between these phenotypes (Fig. 5B).

DISCUSSION

A population of *C. lusitaniae* isolates first described by Demers et al. (10) contained an unexpectedly large number of nonsynonymous mutations in the gene encoding the transcription factor Mrr1, suggesting that Mrr1 activity was under strong selective pressure *in vivo*. These *MRR1* alleles contained either one or two nonsynonymous SNPs or indels (Fig. 1A), and isolates with one mutation had on average higher FLZ resistance than those with two nonsynonymous *MRR1* mutations (Fig. 2A). Deconstruction of *MRR1* alleles with two mutations revealed an evolutionary path in which an activating mutation arose first (e.g., Y1126N) and was followed by suppressing mutations, in the form of premature stop codons, that either restored low basal activity with retention of inducibility [e.g., P1174P(t)], or abolished Mrr1 activity altogether (S359*) (Fig. 3 and see Fig. S3 in the supplemental material). Our findings from the deconstruction of the *MRR1*$^{\mathbf{Y1126N}+P1174P(t)}$ and *MRR1*$^{\mathbf{Y1126N}+S359*}$ alleles (common mutation in bold) led us to propose that similar evolutionary processes likely occurred in lineages containing the L1191H and R1066S mutations (Fig. 1A). It is interesting to note that suppressor mutations only arose in alleles encoding activating mutations affecting the C terminus (Y1126N, L1191H, and R1066S) (see Fig. 2B) and not in alleles with activating mutations affecting the central regulatory domain (e.g., Y813C). This suggests that there may be functional differences between these two types of activating mutations that require future exploration or that these lineages experienced different local environments. Interestingly, a *Candida parapsilosis* strain was recently found to contain a central domain mutation and a premature stop codon (Mrr1$^{P295L+Q1074*}$) similar to the alleles described above, suggesting that selection for and against elevated Mrr1 activity may also occur in other *Candida* species; however, it is not currently known how these individual mutations impact Mrr1 activity and FLZ resistance (66). While previous studies have identified GOF and LOF mutations in genes such as *MRR1*, *TAC1*, *PDR1*, *UPC2*, *ERG3* and *ERG11* that cause increased antifungal resistance (reviewed in references 67 and 68), few instances of sequential mutations in the same gene that cause first an increase then a decrease in activity have been described. Interestingly, multiple studies have shown that alteration in gene copy number, which can be achieved by partial to whole chromosome aneuploidy, can be selected for during stressful conditions and lost upon cessation of the stress, allowing for reversion to a "wild-type" phenotype (reviewed in references 68 and 69). These studies intriguingly parallel our own in that they show both positive and negative selection on a particular phenotype and can result in complex populations with mixed phenotypes. Demers et al. (10) characterized the aneuploidies present in the 20 clinical isolates utilized in these studies; thus far, gene copy number variation has not been determined to be a major driver of antifungal resistance in this *C. lusitaniae* population.

The RNA-Seq analysis of isogenic strains expressing different *MRR1* alleles was consistent with prior studies and showed that *C. lusitaniae* Mrr1 both positively and negatively regulates gene expression (Fig. 1D), although further analysis is required to determine which genes are direct targets of Mrr1. Adding to previous studies in *C. lusitaniae* (10, 29) and *C. albicans* (24), we found that Mrr1 positively regulates 41 genes with a fold change of $\geq$2 and 102 genes with a fold change of $\geq$1.5 (FDR $<$ 0.05). Mrr1-induced genes include multiple MFS and ABC transporters (i.e., *MDR1*, *FLU1*, *CDR1*), methylglyoxal reductases (37), putative alcohol dehydrogenases, and a variety

of other putative metabolic genes (Table S1). Constitutively active Mrr1 also appears to repress expression of 42 genes (fold change $\geq$ 1.5, FDR $<$ 0.05), including multiple iron and/or copper transporters and reductases and sugar transporters (Table S1). These data combined with those from Biermann et al., who showed that *C. lusitaniae* Mrr1 is induced by the spontaneously formed stress signal methylglyoxal (37), imply that Mrr1 may play a larger role in a generalized metabolic or stress response beyond what has been previously studied in response to FLZ and xenobiotic stressors. We propose that potential metabolic differences may account for slight strain-to-strain variability in FLZ MIC when expressing the same *MRR1* variants, such as the subtle difference seen in the U04 and U05 backgrounds when expressing $MRR1^{ancestral}$ and $MRR1^{L1191H+Q1197*}$ (Fig. 1B and C).

The analysis of isogenic and nonisogenic strains showed that the C-terminal region of *C. lusitaniae* Mrr1 is necessary for constitutive Mrr1 activity but not required for induction of Mrr1-regulated genes, such as *MDR1* and *MGD1*, in response to benomyl (Fig. 2D, 3, and S3). Mutations resulting in the loss pf $>$200 amino acids, however, caused strains to phenocopy *mrr1*Δ strains (Fig. 2D and 3C and D). These data are consistent with previous studies showing C-terminal truncations prior to amino acid 944 in *C. albicans MRR1*, homologous to position 1116 in *C. lusitaniae MRR1*, caused a complete loss of *C. albicans* Mrr1 activity (34). Surprisingly, LOF Mrr1 variants and *mrr1*Δ strains showed intermediate expression of a subset of the most strongly differentially regulated genes compared to that of strains with low-activity Mrr1 (Fig. S2B), which has not been observed in other *Candida* species (24, 26, 28). Elevated *MDR1* expression in strains lacking functional Mrr1 caused the unexpectedly high FLZ resistance (Fig. S1A). Though not specifically noted, a slight increase in FLZ resistance was also reported by Kannan et al. (29) upon deletion of *MRR1* from their FLZ-sensitive *C. lusitaniae* isolate P1, supporting our conclusion that this phenomenon spans diverse *C. lusitaniae* isolates. Additional studies are required to determine if this phenomenon is unique to *C. lusitaniae* or is more broadly shared among non-*albicans Candida* species closely related to *C. lusitaniae*, such as *C. auris* (20, 70). Furthermore, while we have shown that the increase in *MDR1* expression in *mrr1*Δ strains is Cap1 independent, additional analyses are required to determine the involvement of other coregulators of the Mrr1 regulon previously described in *C. albicans* (32, 71, 72) and determine if these relationships are conserved in *C. lusitaniae*.

The repeated acquisition of a second mutation in alleles encoding constitutively active Mrr1 variants raised the question as to why, if constitutive Mrr1 was initially selected for, would it later be selected against *in vivo*. From previous studies, it is clear that constitutive Mrr1 activity can be beneficial under a variety of biologically relevant conditions, including exposure to azoles (10, 24), bacterium-produced toxins, including phenazines (10), and host-produced antifungal peptides, including histatin 5 (10, 39). However, little is known about why constitutively active Mrr1 variants would be selected against if there is not a growth defect (Fig. 4A and Fig. S5A). Here, we explored conditions relevant to a chronic lung infection, such as the one these isolates originated from (Fig. 4B). Chronic lung infections are typically an inflamed environment containing a high number of polymorphonuclear leukocytes (PMNs) that produce proteases, myeloperoxidases, and ROS (73, 74), which are important components of the immune system used to kill fungi (reviewed in reference 75). In a screen of diverse chemical compounds, we found that strains with constitutive Mrr1 activity were more strongly inhibited by multiple compounds that have previously been shown to cause damage through oxidative stress (Fig. S5B to D). When we specifically interrogated H_2O_2 resistance, we found that *C. lusitaniae* strains harboring constitutively active Mrr1 variants were more sensitive than strains harboring low-activity Mrr1 variants (Mrr1 ancestral and Mrr1 variants lacking $<$100 amino acids from the C terminus) or lacking a functional Mrr1 (Fig. 4A and S4). Sensitivity to H_2O_2 and the compounds from the Biolog plates was at least partially dependent on Mdr1, though other Mrr1-regulated genes, such as those involved in metabolism, may also contribute to the decreased

growth under conditions of oxidative stress (Fig. S4B, S5, and S6). Interestingly, the trade-off between FLZ and H_2O_2 resistance was conserved in other *Candida* species and among a time series of *C. lusitaniae* isolates (Fig. 4C and 5A).

As outlined in the model in Fig. 5B, together, these data highlight that changing environments within complex and dynamic chronic infections could contribute to the development of heterogeneous fungal populations. Though it appears that the initial selection on the ancestral version of Mrr1 was driven by the need for increased Mrr1 activity, over time, either these selective pressures were removed or other pressures became dominant, resulting in a second mutation in some alleles. In most cases, this secondary wave of mutations caused a decrease or loss of Mrr1 activity that further contributed toward a population with mixed levels of FLZ resistance (Fig. 5B). Although the exact selective pressures at play in this instance are unknown, these data highlight the importance of understanding how microbes evolve *in vivo*, as complex environments, even in the absence of clinically used antifungals, can shape the microbial population and lead to antimicrobial resistance.

MATERIALS AND METHODS

Strains and growth conditions. *Candida* strains used in this study are listed in Table S3 in the supplemental material. All strains were stored as frozen stocks with 25% glycerol at −80°C and subcultured on YPD (1% yeast extract, 2% peptone, 2% glucose, 1.5% agar) plates at 30°C. Strains were regularly grown in YPD liquid medium at 30°C on a roller drum. Cells were grown in YNB (0.67% yeast nitrogen base medium with ammonium sulfate [RPI Corp.]) liquid supplemented with either 2% glucose, 2% glycerol, or 2% Casamino Acids and in RPMI 1640 (Sigma; containing L-glutamine, 165 mM morpholinepropanesulfonic acid [MOPS], 2% glucose) liquid where noted. Medium was supplemented with 8 μg/ml FLZ (stock 4 mg/ml in dimethyl sulfoxide [DMSO]), 1 mM diamide (stock 58 mM in water), or 1 to 6 mM H_2O_2 (30% [wt/vol] in water, ~9.8 M) where noted. *Escherichia coli* strains were grown in LB with either 100 μg/ml carbenicillin or 15 μg/ml gentamicin as necessary to obtain plasmids. BAL fluid and sputum were obtained in accordance with institutional review board protocols as described in reference 76.

DNA for gene knockout constructs. Gene replacement constructs for knocking out *MRR1* (*CLUG_00542*, as annotated in reference 10), *MDR1* (*CLUG_01938/9*, as annotated in reference 10), and *CAP1* (*CLUG_02670*) were generated by fusion PCR as described by Grahl et al. (63). All primers (IDT) used are listed in Table S4. Briefly, 0.5 to 1.0 kb of the 5′ and 3′ regions flanking the gene was amplified from U04 DNA, isolated using the MasterPure yeast DNA purification kit (Epicentre). The codon-optimized nourseothricin (*NAT1* [77]) or hygromycin (*HygB*) resistance cassette was amplified from plasmids pNAT (78) and pYM70 (79), respectively, using the Zyppy plasmid miniprep kit (Zymo Research). Nested primers within the amplified flanking regions were used to stitch the flanks and resistance cassette together. PCR products for transformation were purified and concentrated with the Zymo DNA Clean & Concentrator kit (Zymo Research) with a final elution in molecular biology-grade water (Corning).

DNA for insertion of *NAT1* at neutral site in *C. lusitaniae* genome. The approximately 4,000-bp genomic region between *CLUG_03302* and *CLUG_03303* on chromosome 4, which was not predicted to contain any genes or promoter regions, was targeted as a potentially neutral insertion site. To create plasmid DH3261 containing *NAT1* flanked by homology to this region of chromosome 4, approximately 1.0 kb of the flanking regions (positions 228,652 to 229,651 and 229,701 to 230,691) was amplified from U05 genomic DNA (gDNA). All primers (IDT) used are listed in Table S4. *NAT1* was amplified from pNAT (78). PCR products were purified, concentrated, and then assembled with the vector (pRS426 [80]) linearized with KpnI-HF and SalI-HF (New England BioLabs) and treated with the phosphatase rSAP (New England BioLabs) using the NEBuilder HiFi DNA assembly cloning kit (New England BioLabs). Assemblies were transformed into high-efficiency NEB 5-alpha competent *E. coli* (New England BioLabs). The *NAT1* insertion construct was isolated from DH3261 by digestion with KpnI-HF and SalI-HF (New England BioLabs).

Plasmids for complementation of *MRR1*. Plasmids for complementing *MRR1* were created as described by Biermann et al. (37). For naturally occurring *MRR1* alleles, we amplified (i) the *MRR1* gene and terminator with ~1,150 bp upstream for homology from the appropriate strain's genomic DNA, (ii) the selective marker, *HygB*, from pYM70 (79), and (iii) ~950 bp downstream of *MRR1* for homology from genomic U05 (identical sequence for all relevant strains) using primers (IDT) listed in Table S4. PCR products were cleaned up using the Zymo DNA Clean & Concentrator kit (Zymo Research) and assembled into pMQ30 using the *S. cerevisiae* recombination technique as previously described (81). Plasmids created in *S. cerevisiae* were isolated using a yeast plasmid miniprep kit (Zymo Research) and transformed into high-efficiency NEB 5-alpha competent *E. coli* (New England BioLabs). *E. coli* containing pMQ30-derived plasmids were selected for on LB containing 15 μg/ml gentamicin. Plasmids from *E. coli* were isolated using a Zyppy plasmid miniprep kit (Zymo Research) and subsequently verified by Sanger sequencing at the Dartmouth College Genomics and Molecular Biology Shared Resources Core. pMQ30^{MRR1} complementation plasmids were linearized with NotI-HF (New England BioLabs), cleaned up with the Zymo DNA Clean & Concentrator kit (Zymo Research), and eluted in molecular biology-grade water (Corning) before transformation of ~2 μg into *C. lusitaniae* strain U04 *mrr1*Δ or U05 *mrr1*Δ, as described below.

The *MRR1*^{ancestral} allele sequence was amplified from gDNA of a closely related *C. lusitaniae* isolate (B_L06) that has the same *MRR1* sequence but lacked any of the nonsynonymous mutations that varied among the population of *C. lusitaniae* isolates described here (Fig. 1A). This *MRR1* sequence contains multiple synonymous and nonsynonymous mutations in comparison with that of the reference strain, ATCC 42720 (82). Additional *MRR1* alleles were amplified from gDNA from U04 (*MRR1*^{Y813C}), U05 (*MRR1*$^{L1191H+Q1197*}$), U02 (*MRR1*$^{Y1126N+P1174P(t)}$) and U06 (*MRR1*$^{S359*+Y1126N}$). While making the pMQ30$^{MRR1\text{-}S359*+Y1126N}$ plasmid, one clone was identified that lacked the S359* mutation, resulting in the pMQ30$^{MRR1\text{-}Y1126N}$ plasmid. To create additional *MRR1* alleles that were not identified within any *C. lusitaniae* isolates, pieces of *MRR1* were selectively removed and repaired with DNA either containing or lacking the desired mutation. Because the L1191H and Q1197* mutations were close together, an alternate strategy was used to separate these mutations. DNA fragments synthesized by IDT containing either the L1191H or Q1197* mutations alone (sequences in Table S4) were amplified then assembled with pMQ30$^{MRR1\text{-}L1191H+Q1197*}$ (linearized with PvuI-HF) using the NEBuilder HiFi DNA assembly cloning kit (New England BioLabs). To remove an unexpected nonsynonymous mutation in pMQ30$^{MRR1\text{-}Q1197*}$, this plasmid was digesting with EcoNI and repaired with a piece of DNA amplified from U04 *mrr1*Δ+*MRR1*^{ancestral} lacking the unwanted mutation.

Strain construction. Mutants were constructed as previously described by Grahl et al. using an expression-free ribonucleoprotein CRISPR-Cas9 method (63). Briefly, 1 to 2 μg of DNA for gene knockout constructs generated by PCR or 2 μg of digested plasmid, purified, and concentrated with a final elution in molecular biology-grade water (Corning) was used per transformation. Plasmids containing complementation and knockout constructs and resulting strains are listed in Table S3 and CRISPR RNAs (crRNAs; IDT) are listed in Table S4. Transformants were selected on YPD agar containing 200 μg/ml nourseothricin or 600 μg/ml hygromycin B.

Drug susceptibility assays. MIC was determined using a broth microdilution method as previously described (83) with slight modifications (10). Briefly, 2×10^3 cells were added to a 2-fold dilution series of FLZ prepared in RPMI 1640 medium, testing concentrations from 64 to 0.125 μg/ml, and then incubated at 35°C for 24 h. The MIC was defined as the drug concentration that abolished visible growth compared to that of a drug-free control.

Quantitative RT-PCR. Overnight cultures were back diluted to an optical density at 600 nm (OD_{600}) of ~0.1 and grown for 6 h in YPD liquid medium at 30°C. Then, 50 μg/ml of benomyl (stock 10 mg/ml in DMSO) or an equivalent volume of DMSO was added for experiments assessing the induction of Mrr1 activity; 7.5 μg RNA (harvested using the MasterPure yeast RNA purification kit [Epicentre]) was DNase treated with the Turbo DNA-free kit (Invitrogen). cDNA was synthesized from 300 to 500 ng of DNase-treated RNA using the RevertAid H Minus first-strand cDNA synthesis kit (Thermo Scientific), according to the manufacturer's instructions for random hexamer primer (IDT) and a GC-rich template. Quantitative RT-PCR was performed on a CFX96 real-time system (Bio-Rad), using SsoFast Evergreen supermix (Bio-Rad) with the primers listed in Table S4. Thermocycler conditions were as follows: 95°C for 30 s and 40 cycles of 95°C for 5 s, 65°C for 3 s, and 95°C for 5 s. Transcripts were normalized to *ACT1* expression.

RNA sequencing. Overnight cultures were back diluted into YPD and grown to exponential phase (~8 h) twice and then treated with vehicle or 0.5 mM H_2O_2 for 30 min, in biological triplicates. RNA was harvested from snap-frozen pellets (using liquid nitrogen) using the MasterPure yeast RNA purification kit (Epicentre) and stored at −80°C. RNA libraries were prepared using the Kapa mRNA HyperPrep kit (Roche) and sequenced using single-end 75-bp reads on the Illumina NextSeq 500 platform. The data analysis pipeline is available from the github repository (https://github.com/stajichlab/RNASeq_Clusitaniae_MRR1 and archived as https://www.doi.org/10.5281/zenodo.4477474). FASTQ files were aligned to the ATCC 42720 (82) genome with the splice-site aware and SNP-tolerant short-read aligner GSNAP (v v2019-09-12) (84). The alignments were converted to sorted BAM files with Picard (v2.18.3; https://broadinstitute.github.io/picard/), and read counts were computed with featureCounts (v1.6.2) (85) with updated genome annotation to correct a truncated gene model for locus *CLUG_00542* and combine a single gene split into two, *CLUG_01938_1939*; the reasoning for these changes is explained in reference 10. Differential gene expression analyses were performed with the edgeR (86) package in Bioconductor by fitting a negative binomial linear model. The resulting *P* values were corrected for multiple testing with the Benjamini-Hochberg procedure to control the false-discovery rate. Genes for which there were less than 2 counts per million (CPM) across the three (absent genes) were not included for differentially expressed gene analysis. Two separate linear models, described below, were created to define the Mrr1 regulon under control conditions alone and determine the interaction between Mrr1 activity and H_2O_2 exposure. Heat maps show normalized CPM values that are centered and scaled by gene and hierarchically clustered (Euclidean distance) using pheatmap (87).

To define the Mrr1 regulon in YPD alone, we identified genes differentially expressed between strains with constitutive Mrr1 activity (U04 and U04 *mrr1*Δ+*MRR1*^{Y813C}) and low or no Mrr1 activity (U04 *mrr1*Δ, U04 *mrr1*Δ+*MRR1*^{ancestral}, and U04 *mrr1*Δ+*MRR1*$^{L1191H+Q1197*}$); this model contained 5,474 genes. We discarded genes for which (i) the $\log_2$FC was not greater than 1 (2-fold) (see Fig. 1B) or 0.585 (1.5-fold) (see Table S1) with an FDR of <0.05, (ii) the average CPM for replicates was not greater than 10 for any strain, and (iii) expression in both U04 and U04 *mrr1*Δ+*MRR1*^{Y813C} was not similar. Results are summarized in Table S1, including the Mrr1 regulon as defined here (Table S1A) and the normalized CPM/gene used for this linear model (Table S1B).

To determine how constitutive Mrr1 activity impacted the response to H_2O_2, we identified the overlap between the interaction between U04 or U04 *mrr1*Δ+*MRR1*^{Y813C} and exposure to 0.5 mM H_2O_2, compared to the reference strain (U04 *mrr1*Δ+*MRR1*^{ancestral}) and condition (YPD alone); this model contained 5,600 genes. Results are summarized in Table S2, including the interaction between strains with

constitutively active Mrr1 and H_2O_2 (Table S2A), the effect of H_2O_2 treatment (Table S2B), and all normalized CPM/gene used for this linear model (Table S2C). One U04 *mrr1*Δ and one U04 *mrr1*Δ+*MRR1*^{ancestral} replicate from the 0.5 mM H_2O_2 treatment condition were excluded from heat maps but not statistical analyses, because they displayed signatures not congruent with the rest of the data and did not cluster with other replicates from those strains.

Biolog phenotype MicroArray analysis. The chemicals in Biolog plates PM22D and PM24C were resuspended in 100 μl YPD liquid and transferred to a sterile 96-well polystyrene plate (Fisher). One hundred microliters of cells adjusted to an OD of 0.01 in YPD was added to each well. Plates were incubated at 37°C for 24 h. A control plate containing no drug was grown simultaneously for comparison.

Plate-based chemical sensitivity assays. (i) Serial dilution assays. Following growth in YPD medium overnight with aeration at 30°C, cells were washed and diluted in water to an OD_{600} of 1. Serial dilutions of 10-fold were carried out in a microtiter plate to yield six concentrations ranging from approximately 10^7 cells/ml (for OD_{600} of 1) to approximately 10^2 cells/ml. Five microliters of each dilution was applied to YPD plates containing the designated concentration of H_2O_2, FLZ, or diamide. Images were captured after incubation at 37°C for 24 or 48 h.

(ii) *C. lusitaniae* population screen. Individual isolates were collected from BAL fluid or sputum from the same subject over the course of multiple years; isolates from each sample were saved in a 96-well array format. Isolates were grown in YPD overnight and then transferred to a 384-well plate, with four wells representing each individual isolate. Cultures were spotted onto YPD or YPD supplemented with 8 μg/ml FLZ or 4 mM H_2O_2 using a 384-pin replicator; the screen performed in singlicate. Plates were incubated for 48 h at 37°C. Growth was scored by eye as completely inhibited, partially inhibited, or uninhibited relative to growth on the YPD-only control.

Luminex analysis. Cytokines in BAL fluid samples were measured (pg/ml) in singlicate by Luminex using a Millipore human cytokine multiplex kit (EMD Millipore Corporation, Billerica, MA) according to the manufacturer's instructions. Assays were performed by the DartLab–Immune Monitoring and Flow Cytometry Resource core at Dartmouth.

Statistical analyses. Statistical analyses were performed using GraphPad Prism 9.0.0 (GraphPad Software). Unpaired Student's *t* tests (two-tailed) with Welch's correction were used to evaluate the difference in FLZ MICs between isolates containing one of two mutations in *MRR1*. One and two-way analysis of variance (ANOVA) tests were performed across multiple samples with either Tukey's multiple-comparison test for unpaired analyses or Sidak's multiple-comparison test for paired analyses. *P* values of <0.05 were considered to be significant for all analyses performed and are indicated with asterisks or letters in the text as follows: *, $P < 0.05$; **, $P < 0.01$; ***, $P < 0.001$; ****, $P < 0.0001$. In figures where the statistics are indicated by lowercase letters, samples marked by the same lowercase letter are not significantly different from each other, and samples marked with different lowercase letters are significantly different, as detailed in the figure legends.

Data availability. The data supporting the findings in this study are available within the paper and its supplemental material and are also available from the corresponding author upon request. Whole-genome sequences for strains in Fig. 1A were previously published by Demers et al. (10) and can be found in NCBI under BioProject PRJNA433226. The sequence for *MRR1*^{ancestral}, Sanger sequenced from isolate B_L06, is available in GenBank (MW553730). The raw sequence reads from the RNA-Seq analysis have been deposited into NCBI sequence read archive under BioProject PRJNA680763. Raw and processed RNA-Seq count data are available in Gene Expression Omnibus (GSE162151) and include minor updates to the genome annotation and assembly for *C. lusitaniae*.

SUPPLEMENTAL MATERIAL

Supplemental material is available online only.

FIG S1, TIF file, 0.3 MB.
FIG S2, TIF file, 0.4 MB.
FIG S3, TIF file, 1.0 MB.
FIG S4, PDF file, 2.4 MB.
FIG S5, TIF file, 0.9 MB.
FIG S6, TIF file, 1.4 MB.
TABLE S1, XLSX file, 2.4 MB.
TABLE S2, XLSX file, 6.2 MB.
TABLE S3, DOCX file, 0.1 MB.
TABLE S4, DOCX file, 0.1 MB.

ACKNOWLEDGMENTS

We thank Joachim Morschhäuser and Lawrence Myers for sharing strains, Katja Koeppen for assistance with linear modeling in edgeR, and Amy Biermann for primers.

Research reported in this publication was supported by National Institutes of Health (NIH) grant R01 AI127548 to D.A.H. from the National Institute of Allergy and Infectious Diseases, R01 HL122372 to A.A. from the National Heart, Lung and Blood Institute, and National Institute of General Medical Sciences (NIGMS) of the NIH under award number

T32GM008704 and AI133956 to E.G.D. J.E.S. is a CIFAR Fellow in the program Fungal Kingdom: Threats and Opportunities. This work was also supported by the Cystic Fibrosis Foundation Research Development Program (CFFRDP) STANTO19R0 for the Translational Research Core, P30-DK117469 for the Applied Bioinformatics and Biostatistics Core, and ASHARE20P0 to A.A. Sequencing services and specialized equipment was provided by the Genomics and Molecular Biology Shared Resource Core at Dartmouth, and Luminex analysis was performed by the DartLab–Immune Monitoring and Flow Cytometry Resource Core at Dartmouth, both supported by NCI Cancer Center Support Grant 5P30-CA023108-37. Equipment used was supported by the NIH IDeA award to Dartmouth BioMT P20-GM113132. Analyses were performed using the computational and data storage resources of the University of California-Riverside HPCC funded by grants from the National Science Foundation (NSF) (MRI-1429826) and NIH (1S10OD016290-01A1).

The content is solely the responsibility of the authors and does not necessarily represent the official views of the NIH.

REFERENCES

1. Morley VJ, Woods RJ, Read AF. 2019. Bystander selection for antimicrobial resistance: implications for patient health. Trends Microbiol 27:864–877. https://doi.org/10.1016/j.tim.2019.06.004.
2. Holmes AH, Moore LS, Sundsfjord A, Steinbakk M, Regmi S, Karkey A, Guerin PJ, Piddock LJ. 2016. Understanding the mechanisms and drivers of antimicrobial resistance. Lancet 387:176–187. https://doi.org/10.1016/S0140-6736(15)00473-0.
3. Iwu CD, Korsten L, Okoh AI. 2020. The incidence of antibiotic resistance within and beyond the agricultural ecosystem: a concern for public health. Microbiologyopen 9:e1035. https://doi.org/10.1002/mbo3.1035.
4. Pisoschi AM, Pop A, Georgescu C, Turcuş V, Olah NK, Mathe E. 2018. An overview of natural antimicrobials role in food. Eur J Med Chem 143:922–935. https://doi.org/10.1016/j.ejmech.2017.11.095.
5. Challinor VL, Bode HB. 2015. Bioactive natural products from novel microbial sources. Ann N Y Acad Sci 1354:82–97. https://doi.org/10.1111/nyas.12954.
6. Winstanley C, O'Brien S, Brockhurst MA. 2016. *Pseudomonas aeruginosa* evolutionary adaptation and diversification in cystic fibrosis chronic lung infections. Trends Microbiol 24:327–337. https://doi.org/10.1016/j.tim.2016.01.008.
7. Lieberman TD, Michel JB, Aingaran M, Potter-Bynoe G, Roux D, Davis MR, Jr, Skurnik D, Leiby N, LiPuma JJ, Goldberg JB, McAdam AJ, Priebe GP, Kishony R. 2011. Parallel bacterial evolution within multiple patients identifies candidate pathogenicity genes. Nat Genet 43:1275–1280. https://doi.org/10.1038/ng.997.
8. Lieberman TD, Flett KB, Yelin I, Martin TR, McAdam AJ, Priebe GP, Kishony R. 2014. Genetic variation of a bacterial pathogen within individuals with cystic fibrosis provides a record of selective pressures. Nat Genet 46:82–87. https://doi.org/10.1038/ng.2848.
9. Ciofu O, Lee B, Johannesson M, Hermansen NO, Meyer P, Hoiby N. 2008. Investigation of the *algT* operon sequence in mucoid and non-mucoid *Pseudomonas aeruginosa* isolates from 115 Scandinavian patients with cystic fibrosis and in 88 *in vitro* non-mucoid revertants. Microbiology (Reading) 154:103–113. https://doi.org/10.1099/mic.0.2007/010421-0.
10. Demers EG, Biermann AR, Masonjones S, Crocker AW, Ashare A, Stajich JE, Hogan DA. 2018. Evolution of drug resistance in an antifungal-naive chronic *Candida lusitaniae* infection. Proc Natl Acad Sci U S A 115:12040–-12045. https://doi.org/10.1073/pnas.1807698115.
11. Chen SC, Marriott D, Playford EG, Nguyen Q, Ellis D, Meyer W, Sorrell TC, Slavin M, Australian Candidaemia Study. 2009. Candidaemia with uncommon *Candida* species: predisposing factors, outcome, antifungal susceptibility, and implications for management. Clin Microbiol Infect 15:662–669. https://doi.org/10.1111/j.1469-0691.2009.02821.x.
12. Favel A, Michel-Nguyen A, Peyron F, Martin C, Thomachot L, Datry A, Bouchara JP, Challier S, Noel T, Chastin C, Regli P. 2003. Colony morphology switching of *Candida lusitaniae* and acquisition of multidrug resistance during treatment of a renal infection in a newborn: case report and review of the literature. Diagn Microbiol Infect Dis 47:331–339. https://doi.org/10.1016/S0732-8893(03)00094-4.
13. Asner SA, Giulieri S, Diezi M, Marchetti O, Sanglard D. 2015. Acquired multidrug antifungal resistance in *Candida lusitaniae* during therapy. Antimicrob Agents Chemother 59:7715–7722. https://doi.org/10.1128/AAC.02204-15.
14. Michel RG, Kinasewitz GT, Drevets DA, Levin JH, Warden DW. 2009. Prosthetic valve endocarditis caused by *Candida lusitaniae*, an uncommon pathogen: a case report. J Med Case Rep 3:7611. https://doi.org/10.1186/1752-1947-3-7611.
15. Pietrucha-Dilanchian P, Lewis RE, Ahmad H, Lechin AE. 2001. *Candida lusitaniae* catheter-related sepsis. Ann Pharmacother 35:1570–1574. https://doi.org/10.1345/aph.1A077.
16. Desnos-Ollivier M, Moquet O, Chouaki T, Guerin AM, Dromer F. 2011. Development of echinocandin resistance in *Clavispora lusitaniae* during caspofungin treatment. J Clin Microbiol 49:2304–2306. https://doi.org/10.1128/JCM.00325-11.
17. Hawkins JL, Baddour LM. 2003. *Candida lusitaniae* infections in the era of fluconazole availability. Clin Infect Dis 36:e14–e18. https://doi.org/10.1086/344651.
18. Atkinson BJ, Lewis RE, Kontoyiannis DP. 2008. *Candida lusitaniae* fungemia in cancer patients: risk factors for amphotericin B failure and outcome. Med Mycol 46:541–546. https://doi.org/10.1080/13693780801968571.
19. Reboutier D, Piednoel M, Boisnard S, Conti A, Chevalier V, Florent M, Gibot-Leclerc S, Da Silva B, Chastin C, Fallague K, Favel A, Noel T, Ruprich-Robert G, Chapeland-Leclerc F, Papon N. 2009. Combination of different molecular mechanisms leading to fluconazole resistance in a *Candida lusitaniae* clinical isolate. Diagn Microbiol Infect Dis 63:188–193. https://doi.org/10.1016/j.diagmicrobio.2008.10.019.
20. Shen XX, Zhou X, Kominek J, Kurtzman CP, Hittinger CT, Rokas A. 2016. Reconstructing the backbone of the *Saccharomycotina* yeast phylogeny using genome-scale data. G3 (Bethesda) 6:3927–3939. https://doi.org/10.1534/g3.116.034744.
21. Chow NA, Munoz JF, Gade L, Berkow EL, Li X, Welsh RM, Forsberg K, Lockhart SR, Adam R, Alanio A, Alastruey-Izquierdo A, Althawadi S, Arauz AB, Ben-Ami R, Bharat A, Calvo B, Desnos-Ollivier M, Escandon P, Gardam D, Gunturu R, Heath CH, Kurzai O, Martin R, Litvintseva AP, Cuomo CA. 2020. Tracing the evolutionary history and global expansion of *Candida auris* using population genomic analyses. mBio 11:e03364-19. https://doi.org/10.1128/mBio.03364-19.
22. Du H, Bing J, Hu T, Ennis CL, Nobile CJ, Huang G. 2020. *Candida auris*: epidemiology, biology, antifungal resistance, and virulence. PLoS Pathog 16:e1008921. https://doi.org/10.1371/journal.ppat.1008921.
23. Franz R, Kelly SL, Lamb DC, Kelly DE, Ruhnke M, Morschhauser J. 1998. Multiple molecular mechanisms contribute to a stepwise development of fluconazole resistance in clinical *Candida albicans* strains. Antimicrob Agents Chemother 42:3065–3072. https://doi.org/10.1128/AAC.42.12.3065.
24. Morschhauser J, Barker KS, Liu TT, Bla BWJ, Homayouni R, Rogers PD. 2007. The transcription factor Mrr1p controls expression of the *MDR1* efflux pump and mediates multidrug resistance in *Candida albicans*. PLoS Pathog 3:e164. https://doi.org/10.1371/journal.ppat.0030164.

25. Schubert S, Rogers PD, Morschhauser J. 2008. Gain-of-function mutations in the transcription factor *MRR1* are responsible for overexpression of the *MDR1* efflux pump in fluconazole-resistant *Candida dubliniensis* strains. Antimicrob Agents Chemother 52:4274–4280. https://doi.org/10.1128/AAC.00740-08.
26. Dunkel N, Blass J, Rogers PD, Morschhauser J. 2008. Mutations in the multi-drug resistance regulator *MRR1*, followed by loss of heterozygosity, are the main cause of *MDR1* overexpression in fluconazole-resistant *Candida albicans* strains. Mol Microbiol 69:827–840. https://doi.org/10.1111/j.1365-2958.2008.06309.x.
27. Zhang L, Xiao M, Watts MR, Wang H, Fan X, Kong F, Xu YC. 2015. Development of fluconazole resistance in a series of *Candida parapsilosis* isolates from a persistent candidemia patient with prolonged antifungal therapy. BMC Infect Dis 15:340. https://doi.org/10.1186/s12879-015-1086-6.
28. Branco J, Silva AP, Silva RM, Silva-Dias A, Pina-Vaz C, Butler G, Rodrigues AG, Miranda IM. 2015. Fluconazole and voriconazole resistance in *Candida parapsilosis* is conferred by gain-of-function mutations in *MRR1* transcription factor gene. Antimicrob Agents Chemother 59:6629–6633. https://doi.org/10.1128/AAC.00842-15.
29. Kannan A, Asner SA, Trachsel E, Kelly S, Parker J, Sanglard D. 2019. Comparative genomics for the elucidation of multidrug resistance in *Candida lusitaniae*. mBio 10:e02512-19. https://doi.org/10.1128/mBio.02512-19.
30. Iyer KR, Camara K, Daniel-Ivad M, Trilles R, Pimentel-Elardo SM, Fossen JL, Marchillo K, Liu Z, Singh S, Munoz JF, Kim SH, Porco JA, Jr, Cuomo CA, Williams NS, Ibrahim AS, Edwards JE, Jr, Andes DR, Nodwell JR, Brown LE, Whitesell L, Robbins N, Cowen LE. 2020. An oxindole efflux inhibitor potentiates azoles and impairs virulence in the fungal pathogen *Candida auris*. Nat Commun 11:6429. https://doi.org/10.1038/s41467-020-20183-3.
31. Krugel H, Fiedler G, Haupt I, Sarfert E, Simon H. 1988. Analysis of the nourseothricin-resistance gene (*nat*) of *Streptomyces noursei*. Gene 62:209–217. https://doi.org/10.1016/0378-1119(88)90559-8.
32. Schubert S, Barker KS, Znaidi S, Schneider S, Dierolf F, Dunkel N, Aid M, Boucher G, Rogers PD, Raymond M, Morschhauser J. 2011. Regulation of efflux pump expression and drug resistance by the transcription factors Mrr1, Upc2, and Cap1 in *Candida albicans*. Antimicrob Agents Chemother 55:2212–2223. https://doi.org/10.1128/AAC.01343-10.
33. Rognon B, Kozovska Z, Coste AT, Pardini G, Sanglard D. 2006. Identification of promoter elements responsible for the regulation of *MDR1* from *Candida albicans*, a major facilitator transporter involved in azole resistance. Microbiology (Reading) 152:3701–3722. https://doi.org/10.1099/mic.0.29277-0.
34. Schubert S, Popp C, Rogers PD, Morschhauser J. 2011. Functional dissection of a *Candida albicans* zinc cluster transcription factor, the multidrug resistance regulator Mrr1. Eukaryot Cell 10:1110–1121. https://doi.org/10.1128/EC.05100-11.
35. Karababa M, Coste AT, Rognon B, Bille J, Sanglard D. 2004. Comparison of gene expression profiles of *Candida albicans* azole-resistant clinical isolates and laboratory strains exposed to drugs inducing multidrug transporters. Antimicrob Agents Chemother 48:3064–3079. https://doi.org/10.1128/AAC.48.8.3064-3079.2004.
36. Kwak MK, Ku M, Kang SO. 2018. Inducible NAD(H)-linked methylglyoxal oxidoreductase regulates cellular methylglyoxal and pyruvate through enhanced activities of alcohol dehydrogenase and methylglyoxal-oxidizing enzymes in glutathione-depleted *Candida albicans*. Biochim Biophys Acta Gen Subj 1862:18–39. https://doi.org/10.1016/j.bbagen.2017.10.003.
37. Biermann AR, Demers EG, Hogan DA. 2020. Mrr1 regulation of methylglyoxal catabolism and methylglyoxal-induced fluconazole resistance in *Candida lusitaniae*. Mol Microbiol 115:116–130. https://doi.org/10.1111/mmi.14604.
38. Calabrese D, Bille J, Sanglard D. 2000. A novel multidrug efflux transporter gene of the major facilitator superfamily from *Candida albicans* (*FLU1*) conferring resistance to fluconazole. Microbiology 146:2743–2754. https://doi.org/10.1099/00221287-146-11-2743.
39. Hampe IAI, Friedman J, Edgerton M, Morschhauser J. 2017. An acquired mechanism of antifungal drug resistance simultaneously enables *Candida albicans* to escape from intrinsic host defenses. PLoS Pathog 13:e1006655. https://doi.org/10.1371/journal.ppat.1006655.
40. Alonso A, Martinez JL. 2001. Expression of multidrug efflux pump SmeDEF by clinical isolates of *Stenotrophomonas maltophilia*. Antimicrob Agents Chemother 45:1879–1881. https://doi.org/10.1128/AAC.45.6.1879-1881.2001.
41. Praski Alzrigat L, Huseby DL, Brandis G, Hughes D. 2017. Fitness cost constrains the spectrum of *marR* mutations in ciprofloxacin-resistant *Escherichia coli*. J Antimicrob Chemother 72:3016–3024. https://doi.org/10.1093/jac/dkx270.
42. Popp C, Hampe IAI, Hertlein T, Ohlsen K, Rogers PD, Morschhauser J. 2017. Competitive fitness of fluconazole-resistant clinical *Candida albicans* strains. Antimicrob Agents Chemother 61:e00584-17. https://doi.org/10.1128/AAC.00584-17.
43. Rottner M, Freyssinet JM, Martinez MC. 2009. Mechanisms of the noxious inflammatory cycle in cystic fibrosis. Respir Res 10:23. https://doi.org/10.1186/1465-9921-10-23.
44. Laval J, Ralhan A, Hartl D. 2016. Neutrophils in cystic fibrosis. Biol Chem 397:485–496. https://doi.org/10.1515/hsz-2015-0271.
45. Moran GP, Sanglard D, Donnelly SM, Shanley DB, Sullivan DJ, Coleman DC. 1998. Identification and expression of multidrug transporters responsible for fluconazole resistance in *Candida dubliniensis*. Antimicrob Agents Chemother 42:1819–1830. https://doi.org/10.1128/AAC.42.7.1819.
46. Moran GP, Sullivan DJ, Henman MC, McCreary CE, Harrington BJ, Shanley DB, Coleman DC. 1997. Antifungal drug susceptibilities of oral *Candida dubliniensis* isolates from human immunodeficiency virus (HIV)-infected and non-HIV-infected subjects and generation of stable fluconazole-resistant derivatives *in vitro*. Antimicrob Agents Chemother 41:617–623. https://doi.org/10.1128/AAC.41.3.617.
47. Ludewig G, Williams JM, Li Y, Staben C. 1994. Effects of pentamidine isethionate on *Saccharomyces cerevisiae*. Antimicrob Agents Chemother 38:1123–1128. https://doi.org/10.1128/aac.38.5.1123.
48. Cox LJ, Dooley D, Beumer R. 1990. Effect of lithium chloride and other inhibitors on the growth of *Listeria* spp. Food Microbiol 7:311–325. https://doi.org/10.1016/0740-0020(90)90036-H.
49. Murry R, Kniemeyer O, Krause K, Saiardi A, Kothe E. 2019. Crosstalk between Ras and inositol phosphate signaling revealed by lithium action on inositol monophosphatase in *Schizophyllum commune*. Adv Biol Regul 72:78–88. https://doi.org/10.1016/j.jbior.2019.01.001.
50. Xu Y, Wang Y, Yan L, Liang RM, Dai BD, Tang RJ, Gao PH, Jiang YY. 2009. Proteomic analysis reveals a synergistic mechanism of fluconazole and berberine against fluconazole-resistant *Candida albicans*: endogenous ROS augmentation. J Proteome Res 8:5296–5304. https://doi.org/10.1021/pr9005074.
51. Dhamgaye S, Devaux F, Vandeputte P, Khandelwal NK, Sanglard D, Mukhopadhyay G, Prasad R. 2014. Molecular mechanisms of action of herbal antifungal alkaloid berberine, in *Candida albicans*. PLoS One 9:e104554. https://doi.org/10.1371/journal.pone.0104554.
52. Henderson G. 1989. A comparison of the effects of chromate, molybdate and cadmium oxide on respiration in the yeast *Saccharomyces cerevisiae*. Biol Met 2:83–88. https://doi.org/10.1007/BF01129205.
53. Jouaville LS, Pinton P, Bastianutto C, Rutter GA, Rizzuto R. 1999. Regulation of mitochondrial ATP synthesis by calcium: evidence for a long-term metabolic priming. Proc Natl Acad Sci U S A 96:13807–13812. https://doi.org/10.1073/pnas.96.24.13807.
54. Edwards KJ, Jenkins TC, Neidle S. 1992. Crystal structure of a pentamidine-oligonucleotide complex: implications for DNA-binding properties. Biochemistry 31:7104–7109. https://doi.org/10.1021/bi00146a011.
55. Lerman LS. 1961. Structural considerations in the interaction of DNA and acridines. J Mol Biol 3:18–30. https://doi.org/10.1016/s0022-2836(61)80004-1.
56. Krey AK, Hahn FE. 1969. Berberine: complex with DNA. Science 166:755–757. https://doi.org/10.1126/science.166.3906.755.
57. Exinger F, Lacroute F. 1992. 6-Azauracil inhibition of GTP biosynthesis in *Saccharomyces cerevisiae*. Curr Genet 22:9–11. https://doi.org/10.1007/BF00351735.
58. Handschumacher RE. 1960. Orotidylic acid decarboxylase: inhibition studies with azauridine 5'-phosphate. J Biol Chem 235:2917–2919. https://doi.org/10.1016/S0021-9258(18)64562-4.
59. Bridgewater LC, Manning FC, Patierno SR. 1994. Base-specific arrest of *in vitro* DNA replication by carcinogenic chromium: relationship to DNA interstrand crosslinking. Carcinogenesis 15:2421–2427. https://doi.org/10.1093/carcin/15.11.2421.
60. da Silva AR, de Andrade Neto JB, da Silva CR, Campos R. d S, Costa Silva RA, Freitas DD, do Nascimento FBSA, de Andrade LND, Sampaio LS, Grangeiro TB, Magalhães HIF, Cavalcanti BC, de Moraes MO, Nobre Júnior HV. 2016. Berberine antifungal activity in fluconazole-resistant pathogenic yeasts: action mechanism evaluated by flow cytometry and biofilm growth inhibition in *Candida* spp. Antimicrob Agents Chemother 60:3551–3557. https://doi.org/10.1128/AAC.01846-15.
61. Liu S, Yue L, Gu W, Li X, Zhang L, Sun S. 2016. Synergistic effect of fluconazole and calcium channel blockers against resistant *Candida albicans*. PLoS One 11:e0150859. https://doi.org/10.1371/journal.pone.0150859.
62. Kaur R, Castano I, Cormack BP. 2004. Functional genomic analysis of fluconazole susceptibility in the pathogenic yeast *Candida glabrata*: roles of

calcium signaling and mitochondria. Antimicrob Agents Chemother 48:1600–1613. https://doi.org/10.1128/aac.48.5.1600-1613.2004.
63. Grahl N, Demers EG, Crocker AW, Hogan DA. 2017. Use of RNA-protein complexes for genome editing in non-*albicans Candida* species. mSphere 2:e00218-17. https://doi.org/10.1128/mSphere.00218-17.
64. Enjalbert B, Nantel A, Whiteway M. 2003. Stress-induced gene expression in *Candida albicans*: absence of a general stress response. Mol Biol Cell 14:1460–1467. https://doi.org/10.1091/mbc.e02-08-0546.
65. Enjalbert B, Smith DA, Cornell MJ, Alam I, Nicholls S, Brown AJ, Quinn J. 2006. Role of the Hog1 stress-activated protein kinase in the global transcriptional response to stress in the fungal pathogen *Candida albicans*. Mol Biol Cell 17:1018–1032. https://doi.org/10.1091/mbc.e05-06-0501.
66. Arastehfar A, Daneshnia F, Hilmioğlu-Polat S, Fang W, Yaşar M, Polat F, Metin DY, Rigole P, Coenye T, Ilkit M, Pan W, Liao W, Hagen F, Kostrzewa M, Perlin DS, Lass-Flörl C, Boekhout T. 2020. First report of candidemia clonal outbreak caused by emerging fluconazole-resistant *Candida parapsilosis* isolates harboring Y132F and/or Y132F+K143R in Turkey. Antimicrob Agents Chemother 64:e01001-20. https://doi.org/10.1128/AAC.01001-20.
67. Lee Y, Puumala E, Robbins N, Cowen LE. 22 May 2020. Antifungal drug resistance: molecular mechanisms in *Candida albicans* and beyond. Chem Rev https://doi.org/10.1021/acs.chemrev.0c00199.
68. Berman J, Krysan DJ. 2020. Drug resistance and tolerance in fungi. Nat Rev Microbiol 18:319–331. https://doi.org/10.1038/s41579-019-0322-2.
69. Gilchrist C, Stelkens R. 2019. Aneuploidy in yeast: segregation error or adaptation mechanism? Yeast 36:525–539. https://doi.org/10.1002/yea.3427.
70. Munoz JF, Gade L, Chow NA, Loparev VN, Juieng P, Berkow EL, Farrer RA, Litvintseva AP, Cuomo CA. 2018. Genomic insights into multidrug-resistance, mating and virulence in *Candida auris* and related emerging species. Nat Commun 9:5346. https://doi.org/10.1038/s41467-018-07779-6.
71. Liu Z, Myers LC. 2017. *Candida albicans* Swi/Snf and mediator complexes differentially regulate Mrr1-induced *MDR1* expression and fluconazole resistance. Antimicrob Agents Chemother 61:e01344-17. https://doi.org/10.1128/AAC.01344-17.
72. Mogavero S, Tavanti A, Senesi S, Rogers PD, Morschhauser J. 2011. Differential requirement of the transcription factor Mcm1 for activation of the *Candida albicans* multidrug efflux pump *MDR1* by its regulators Mrr1 and Cap1. Antimicrob Agents Chemother 55:2061–2066. https://doi.org/10.1128/AAC.01467-10.
73. Hull J, Vervaart P, Grimwood K, Phelan P. 1997. Pulmonary oxidative stress response in young children with cystic fibrosis. Thorax 52:557–560. https://doi.org/10.1136/thx.52.6.557.
74. Brown RK, Kelly FJ. 1994. Evidence for increased oxidative damage in patients with cystic fibrosis. Pediatr Res 36:487–493. https://doi.org/10.1203/00006450-199410000-00013.
75. Warris A, Ballou ER. 2019. Oxidative responses and fungal infection biology. Semin Cell Dev Biol 89:34–46. https://doi.org/10.1016/j.semcdb.2018.03.004.
76. Hogan DA, Willger SD, Dolben EL, Hampton TH, Stanton BA, Morrison HG, Sogin ML, Czum J, Ashare A. 2016. Analysis of lung microbiota in bronchoalveolar lavage, protected brush and sputum samples from subjects with mild-to-moderate cystic fibrosis lung disease. PLoS One 11:e0149998. https://doi.org/10.1371/journal.pone.0149998.
77. Shen J, Guo W, Kohler JR. 2005. *CaNAT1*, a heterologous dominant selectable marker for transformation of *Candida albicans* and other pathogenic *Candida* species. Infect Immun 73:1239–1242. https://doi.org/10.1128/IAI.73.2.1239-1242.2005.
78. Min K, Ichikawa Y, Woolford CA, Mitchell AP. 2016. *Candida albicans* gene deletion with a transient CRISPR-Cas9 system. mSphere 1:e00130-16. https://doi.org/10.1128/mSphere.00130-16.
79. Basso LR, Jr, Bartiss A, Mao Y, Gast CE, Coelho PS, Snyder M, Wong B. 2010. Transformation of *Candida albicans* with a synthetic hygromycin B resistance gene. Yeast 27:1039–1048. https://doi.org/10.1002/yea.1813.
80. Christianson TW, Sikorski RS, Dante M, Shero JH, Hieter P. 1992. Multifunctional yeast high-copy-number shuttle vectors. Gene 110:119–122. https://doi.org/10.1016/0378-1119(92)90454-w.
81. Shanks RM, Caiazza NC, Hinsa SM, Toutain CM, O'Toole GA. 2006. *Saccharomyces cerevisiae*-based molecular tool kit for manipulation of genes from gram-negative bacteria. Appl Environ Microbiol 72:5027–5036. https://doi.org/10.1128/AEM.00682-06.
82. Butler G, Rasmussen MD, Lin MF, Santos MAS, Sakthikumar S, Munro CA, Rheinbay E, Grabherr M, Forche A, Reedy JL, Agrafioti I, Arnaud MB, Bates S, Brown AJP, Brunke S, Costanzo MC, Fitzpatrick DA, de Groot PWJ, Harris D, Hoyer LL, Hube B, Klis FM, Kodira C, Lennard N, Logue ME, Martin R, Neiman AM, Nikolaou E, Quail MA, Quinn J, Santos MC, Schmitzberger FF, Sherlock G, Shah P, Silverstein KAT, Skrzypek MS, Soll D, Staggs R, Stansfield I, Stumpf MPH, Sudbery PE, Srikantha T, Zeng Q, Berman J, Berriman M, Heitman J, Gow NAR, Lorenz MC, Birren BW, Kellis M, et al. 2009. Evolution of pathogenicity and sexual reproduction in eight *Candida* genomes. Nature 459:657–662. https://doi.org/10.1038/nature08064.
83. CLSI. 2012. Reference method for broth dilution antifungal susceptibility testing of yeasts; CLSI document M27-S4. Clinical and Laboratory Standards Institute, Wayne, PA.
84. Wu TD, Reeder J, Lawrence M, Becker G, Brauer MJ. 2016. GMAP and GSNAP for genomic sequence alignment: enhancements to speed, accuracy, and functionality. Methods Mol Biol 1418:283–334. https://doi.org/10.1007/978-1-4939-3578-9_15.
85. Liao Y, Smyth GK, Shi W. 2014. featureCounts: an efficient general purpose program for assigning sequence reads to genomic features. Bioinformatics 30:923–930. https://doi.org/10.1093/bioinformatics/btt656.
86. Robinson MD, McCarthy DJ, Smyth GK. 2010. edgeR: a Bioconductor package for differential expression analysis of digital gene expression data. Bioinformatics 26:139–140. https://doi.org/10.1093/bioinformatics/btp616.
87. Kolde R 2019. pheatmap: Pretty heatmaps. R package version 1.0.12. https://rdrr.io/cran/pheatmap/.